to the components of the metabolic syndrome and biomarkers of endothelial dysfunction in youth. Diabetes Care 30:2091–2097
72. **Sunehag AL, Toffolo G, Treuth MS, Butte NF, Cobelli C, Bier DM, Haymond MW** 2002 Effects of dietary macronutrient content on glucose metabolism in children. J Clin Endocrinol Metab 87:5168–5178
73. **Galgani JE, Uauy RD, Aguirre CA, Díaz EO** 2008 Effect of the dietary fat quality on insulin sensitivity. Br J Nutr 100:471–479
74. **Steffen LM, Jacobs Jr DR, Murtaugh MA, Moran A, Steinberger J, Hong CP, Sinaiko AR** 2003 Whole grain intake is associated with lower body mass and greater insulin sensitivity among adolescents. Am J Epidemiol 158:243–250
75. **Smith RN, Mann NJ, Braue A, Mäkeläinen H, Varigos GA** 2007 A low-glycemic-load diet improves symptoms in acne vulgaris patients: a randomized controlled trial. Am J Clin Nutr 86:107–115
76. **Ebbeling CB, Leidig MM, Sinclair KB, Hangen JP, Ludwig DS** 2003 A reduced-glycemic load diet in the treatment of adolescent obesity. Arch Pediatr Adolesc Med 157:773–779
77. **Thomas DE, Elliott EJ, Baur L** 2007 Low glycaemic index or low glycaemic load diets for overweight and obesity. Cochrane Database Syst Rev CD005105
78. **Berkowitz RI, Wadden TA, Tershakovec AM, Cronquist JL** 2003 Behavior therapy and sibutramine for the treatment of adolescent obesity: a randomized controlled trial. JAMA 289:1805–1812
79. **McDuffie JR, Calis KA, Uwaifo GI, Sebring NG, Fallon EM, Hubbard VS, Yanovski JA** 2002 Three-month tolerability of orlistat in adolescents with obesity-related comorbid conditions. Obes Res 10:642–650
80. **McDuffie JR, Calis KA, Uwaifo GI, Sebring NG, Fallon EM, Frazer TE, Van Hubbard S, Yanovski JA** 2004 Efficacy of orlistat as an adjunct to behavioral treatment in overweight African American and Caucasian adolescents with obesity-related co-morbid conditions. J Pediatr Endocrinol Metab 17:307–319
81. **Carrel AL, Clark RR, Peterson SE, Nemeth BA, Sullivan J, Allen DB** 2005 Improvement of fitness, body composition, and insulin sensitivity in overweight children in a school-based exercise program: a randomized, controlled study. Arch Pediatr Adolesc Med 159:963–968
82. **Ferguson MA, Gutin B, Le NA, Karp W, Litaker M, Humphries M, Okuyama T, Riggs S, Owens S** 1999 Effects of exercise training and its cessation on components of the insulin resistance syndrome in obese children. Int J Obes Relat Metab Disord 23:889–895
83. **Balagopal P, George D, Patton N, Yarandi H, Roberts WL, Bayne E, Gidding S** 2005 Lifestyle-only intervention attenuates the inflammatory state associated with obesity: a randomized controlled study in adolescents. J Pediatr 146:342–348
84. **Allen DB, Nemeth BA, Clark RR, Peterson SE, Eickhoff J, Carrel AL** 2007 Fitness is a stronger predictor of fasting insulin levels than fatness in overweight male middle-school children. J Pediatr 150:383–387
85. **Nassis GP, Papantakou K, Skenderi K, Triandafillopoulou M, Kavouras SA, Yannakoulia M, Chrousos GP, Sidossis LS** 2005 Aerobic exercise training improves insulin sensitivity without changes in body weight, body fat, adiponectin, and inflammatory markers in overweight and obese girls. Metabolism 54:1472–1479
86. **Bell LM, Watts K, Siafarikas A, Thompson A, Ratnam N, Bulsara M, Finn J, O'Driscoll G, Green DJ, Jones TW, Davis EA** 2007 Exercise alone reduces insulin resistance in obese children independently of changes in body composition. J Clin Endocrinol Metab 92:4230–4235
87. **Savoye M, Shaw M, Dziura J, Tamborlane WV, Rose P, Guandalini C, Goldberg-Gell R, Burgert TS, Cali AM, Weiss R, Caprio S** 2007 Effects of a weight management program on body composition and metabolic parameters in overweight children: a randomized controlled trial. JAMA 297:2697–2704
88. **Park TG, Hong HR, Lee J, Kang HS** 2007 Lifestyle plus exercise intervention improves metabolic syndrome markers without change in adiponectin in obese girls. Ann Nutr Metab 51:197–203
89. **Jones KL, Arslanian S, Peterokova VA, Park JS, Tomlinson MJ** 2002 Effect of metformin in pediatric patients with type 2 diabetes: a randomized controlled trial. Diabetes Care 25:89–94
90. **Arslanian SA, Lewy V, Danadian K, Saad R** 2002 Metformin therapy in obese adolescents with polycystic ovary syndrome and impaired glucose tolerance: amelioration of exaggerated adrenal response to adrenocorticotropin with reduction of insulinemia/insulin resistance. J Clin Endocrinol Metab 87:1555–1559
91. **Gungor N, Arslanian S** 2002 Pathophysiology of type 2 diabetes mellitus in children and adolescents: treatment implications. Treat Endocrinol 1:359–371
92. **Gottschalk M, Danne T, Vlajnic A, Cara JF** 2007 Glimepiride versus metformin as monotherapy in pediatric patients with type 2 diabetes. Diabetes Care 30:790–794
93. **Rotteveel J, van Weissenbruch MM, Twisk JW, Delemarre-Van de Waal HA** 2008 Infant and childhood growth patterns, insulin sensitivity, and blood pressure in prematurely born young adults. Pediatrics 122:313–321
94. **Bhargava SK, Sachdev HS, Fall CH, Osmond C, Lakshmy R, Barker DJ, Biswas SK, Ramji S, Prabhakaran D, Reddy KS** 2004 Relation of serial changes in childhood body-mass index to impaired glucose tolerance in young adulthood. N Engl J Med 350:865–875
95. **Jago R, Wedderkopp N, Kristensen PL, Møller NC, Andersen LB, Cooper AR, Froberg K** 2008 Six-year change in youth physical activity and effect on fasting insulin and HOMA-IR. Am J Prev Med 35:554–560
96. **Bridger T, MacDonald S, Baltzer F, Rodd C** 2006 Randomized placebo-controlled trial of metformin for adolescents with polycystic ovary syndrome. Arch Pediatr Adolesc Med 160:241–246
97. **Ibáñez L, Ong K, Ferrer A, Amin R, Dunger D, de Zegher F** 2003 Low-dose flutamide-metformin therapy reverses insulin resistance and reduces fat mass in nonobese adolescents with ovarian hyperandrogenism. J Clin Endocrinol Metab 88:2600–2606
98. **Ibáñez L, de Zegher F** 2006 Low-dose flutamide-metformin therapy for hyperinsulinemic hyperandrogenism in non-obese adolescents and women. Hum Reprod Update 12:243–252
99. **Plagemann A, Harder T, Kohlhoff R, Rohde W, Dörner G** 1997 Glucose tolerance and insulin secretion in children of mothers with pregestational IDDM or gestational diabetes. Diabetologia 40:1094–1100
100. **Dabelea D, Hanson RL, Lindsay RS, Pettitt DJ, Imperatore G, Gabir MM, Roumain J, Bennett PH, Knowler WC** 2000 Intrauterine exposure to diabetes conveys risks for type 2 diabetes and obesity: a study of discordant sibships. Diabetes 49:2208–2211
101. **Oken E, Levitan EB, Gillman MW** 2008 Maternal smoking during pregnancy and child overweight: systematic review and meta-analysis. Int J Obes (Lond) 32:201–210
102. **Kinra S, Rameshwar Sarma KV, Ghafoorunissa, Mendu VV, Ravikumar R, Mohan V, Wilkinson IB, Cockcroft JR, Davey Smith G, Ben-Shlomo Y** 2008 Effect of integration of supplemental nutrition with public health programmes in pregnancy and early childhood on cardiovascular risk in rural Indian adolescents: long term follow-up of Hyderabad nutrition trial. BMJ 337:a605
103. **Harder T, Bergmann R, Kallischnigg G, Plagemann A** 2005 Duration of breastfeeding and risk of overweight: a meta-analysis. Am J Epidemiol 162:397–403
104. **Koletzko B, von Kries R, Closa R, Monasterolo RC, Escribano J, Subías JE, Scaglioni S, Giovannini M, Beyer J, Demmelmair H, Anton B, Gruszfeld D, Dobrzanska A, Sengier A, Langhendries JP, Rolland Cachera MF, Grote V** 2009 Can infant feeding choices modulate later obesity risk? Am J Clin Nutr 89:1502S–1508S
105. **Kaitosaari T, Rönnemaa T, Viikari J, Raitakari O, Arffman M, Marniemi J, Kallio K, Pahkala K, Jokinen E, Simell O** 2006 Low-saturated fat dietary counseling starting in infancy improves insulin sensitivity in 9-year-old healthy children: the Special Turku Coronary Risk Factor Intervention Project for Children (STRIP) study. Diabetes Care 29:781–785

ACTA PÆDIATRICA
NURTURING THE CHILD

Acta Pædiatrica ISSN 0803–5253

REGULAR ARTICLE

Impact of leptin and leptin-receptor gene polymorphisms on serum lipids in Japanese obese children

T Okada (tomokada@med.nihon-u.ac.jp)[1], T Ohzeki[2], Y Nakagawa[2], S Sugihara[3], O Arisaka[4], The Study Group of Pediatric Obesity and Its related Metabolism

1.Department of Pediatrics and Child Health, Nihon University School of Medicine, Tokyo, Japan
2.Department of Pediatrics, Hamamatsu University School of Medicine, Shizuoka, Japan
3.Department of Pediatrics, Tokyo Women's Medical University Medical Center East, Tokyo, Japan
4.Department of Pediatrics, Dokkyo University School of Medicine, Tochigi, Japan

Keywords
Leptin gene, Leptin receptor gene, Obese children, Polymorphism

Correspondence
T Okada, M.D., Department of Pediatrics and Child Health, Nihon University School of Medicine 30-1, Oyaguchi Kamicho, Itabashi-ku 173-8610, Tokyo, Japan.
Tel: +81-3-3972-8111 |
Fax: +81-3-3957-6186 |
Email: tomokada@med.nihon-u.ac.jp

Received
3 October 2009; revised 28 January 2010; accepted 17 February 2010.

DOI:10.1111/j.1651-2227.2010.01778.x

Abstract

Aim: Leptin is one of the factors affecting serum lipid profile. We investigated the association between serum lipids and leptin/leptin receptor (LEPR) gene polymorphisms in obese Japanese children.

Methods: One hundred and thirty-six obese children (99 males and 37 females, relative weight over than 20%) from 5 to 17 years of age were recruited from 10 institutes. Four known polymorphisms in leptin gene [(+19)A G, (−2548)G A, (−188)C A, (−633)C T] and four known polymorphisms in LEPR gene [Lys109Arg, Gln223Arg, Pro(G)1019Pro(A), Ser(T)343Ser(C)] were determined using polymerase chain reaction-restriction fragment length polymorphism-based analyses.

Results: No associations were found between leptin gene polymorphisms and serum lipid profile. On the other hand, Lys109Arg and Ser343Ser polymorphism in LEPR gene, but not Gln223Arg or Pro1019Pro, had significant relationships with serum lipid profile; lower total and low-density lipoprotein cholesterol levels in Arg109Arg homozygotes, and lower TG levels in Ser343Ser(C/C) homozygotes. In addition, LEPR gene also associated with relative weight; Arg109Arg homozygotes had higher relative weight and Ser343Ser(C/C) homozygotes had lower one.

Conclusion: These results suggest that LEPR gene polymorphisms may partly contribute to serum lipid profile in obese children.

INTRODUCTION

The recent rapid increase in the prevalence of obesity is undoubtedly caused by changes in life-style such as diet and physical activity. However, the individual susceptibility to these changes depends on some factors including genetic predisposition (1). The genetic contribution to control body weight in humans has been investigated by family studies, especially in twins (2–5), demonstrating that genetic factors account for 20–60% of the variation in body weight. In addition, this effect is presumed to be polygenic in origin (6). However, it has been confirmed that several single genes in the leptin-melanocortin pathway have a profound effect on the development of early-onset severe obesity (7). Leptin, an adipocyte-derived hormone, regulates body weight and energy expenditure as a result of both anorectic effects and metabolic effects (8). Leptin acts via leptin receptor (LEPR), which is expressed predominantly in hypothalamus but is also widely distributed in most peripheral tissues. Mutations in genes encoding leptin/LEPR resulting in leptin/LEPR deficiency have been reported in severely obese children (9). These abnormalities, however, are extremely rare and thus cannot explain the genetic predisposition for common human obesity. By contrast, several polymorphisms of leptin/LEPR genes are commonly demonstrated in humans (10).

Many epidemiological and clinical studies have been performed to investigate the association between leptin/LEPR gene polymorphisms and obesity, demonstrating the limited influence of the gene polymorphisms (10,11). In Japanese, the effect of leptin gene polymorphisms on obesity is controversial (12,13), and no association was found between LEPR gene polymorphisms and obesity (14–18). Several studies in humans, however, demonstrated that some LEPR gene polymorphisms had significant influences on complications of obesity, such as hypertension (19), glucose intolerance (17) or sleep apnea syndrome (20). Leptin also has a profound influence on serum lipid levels through both central and peripheral actions (21,22). The previous studies have shown the significant association of LEPR gene polymorphisms with serum lipids (20,23,24). However, only the limited information is provided in this field. Therefore, we investigated the impact of leptin/LEPR gene polymorphisms on serum lipid profile in obese children in this study. In children, the phenotypic presentation caused by gene polymorphisms may be more obvious, because they have less influenced by life-style related environmental factors.

MATERIALS AND METHODS

Subjects

A total of 136 obese children (99 males and 37 females) from 5 to 17 years of age were recruited from outpatient clinics of 10 institutes in Japan (mean relative weight ± SE was 156.2 ± 2.1%, that ranges from 120.5 to 269.4%). Obesity was defined as relative body weight greater than 120% for children, calculated according to the standard weight for sex, age and height. Children with short stature (below −2.0 SD for age and sex) and/or endogen obesity were excluded. Informed consent was obtained from the children and their parents before participation in this study. The study protocol was approved by the ethics committee of each institute.

Measurements

Blood sample was obtained during 9–11 in the morning after overnight fasting. Total cholesterol (TC), high density lipoprotein cholesterol (HDL-C) and triglyceride (TG) levels are measured using enzymatic methods. Low density lipoprotein cholesterol (LDL-C) levels were obtained using the Friedewald formula (25).

Polymorphism analysis

Genomic DNA was extracted from peripheral blood leucocytes. The four leptin gene polymorphisms, (+19)A → G, (−2548)G → A, (−188)C → A and (−633)C → T, and four LEPR gene polymorphisms, Lys109Arg, Gln223Arg, Pro(G)1019Pro(A), Ser(T)343Ser(C), were determined using a polymerase chain reaction (PCR)-restriction fragment length polymorphism (RFLP)-based analyses. The sequences of primer pairs and restriction endonucleases are listed in Table 1.

Statistical analysis

Data are expressed as mean ± standard error. Differences among gene polymorphism groups were analysed using Kruskal–Wallis test. A chi-squared test was used to analyse the distributions of the gene polymorphisms in groups. To analyse the interaction of gene polymorphisms and relative weight, multiple regression analyses were employed. A p-value below 0.05 was considered statistically significant. Statistical analyses were conducted using the statistical package STATVIEW (ver. 4.5; Abacus Concepts, Berkeley, CA, USA).

RESULTS

Characteristics of the study population

According to the criteria of normal serum lipid levels for Japanese children (26,27), 19 children (14.0%; 13 males and 6 females) had hypercholesterolaemia (>220 mg/dL), 36 (26.5%; 24 males and 12 females) had borderline levels of TC (190–219 mg/dL), 19 (14.0%; 15 male and 4 female) had low HDL-C levels (<40 mg/dL), and 32 (23.5%; 18 males and 14 females) had hypertriglyceridaemia (>140 mg/dL). We found one child with TG levels over 400 mg/dL, thus its LDL-C levels could not be obtained using the Friedewald formula. Twenty-one children (15.6%; 14 males and 7 females) had high LDL-C levels (>140 mg/dL) and 39 (28.9%; 30 males and 9 females) had borderline levels (110–139 mg/dL).

Polymorphisms in leptin and leptin receptor genes

In the present subjects, the genotype distribution of leptin/LEPR genes was shown in Table 2. We found no children with polymorphism of (−188) C –> A or (−633) C –> T in leptin gene. In (+19)A–>G and (−2548)G–>A locus of leptin gene, however, about two-third was demonstrated to be mutant homozygotes. While, in LEPR gene, we also found that about two-third of the obese children had Arg109Arg, Arg223Arg and Pro1019Pro(A/A), and, by contrast, only 15.4% of the subjects had Ser343Ser(C/C).

Table 1 Sequences of primer pairs and endonucleases for polymorphism analyses

	Oligonucleotide primer	Restriction endonuclease
Leptin gene polymorphism		
(+19)A → G	5′-TGATCGGGCCGCTATAAGAG-3′ 5′-AGGAGGAAGGAGCGCGCC-3′	MspA1 I
(−2548)G → A	5′-TTTCCTGTAATTTTCCCGTGAG-3′ 5′-AAAGCAAAGACAGGCATAAAAA-3′	Hha I
(−188)C → A	5′-CAACGAGGGCGCAGCCGTAT-3′ 5′-CGCATTTCTAGCGCCAGCTC-3′	BssH II
(−633)C → T	5′-TGGGACCACCCCCCAACCCCCACTTTGTAC-3′ 5′-AAGTTGTCTCTGGCTGGCACCCCAGGGAGTGCGC-3′	BssH II
Leptin receptor gene polymorphism		
Lys(G)109Arg(A)	5′-TTTCCACTGTTGCTTTCGGA-3′ 5′-AAACTAAAGAATTTACTGTTGAAACAAATGGC-3′	Hae III
Gln(G)223Arg(A)	5′-ACCCTTTAAGCTGGGTGTCCCAAATAG-3′ 5′-AGCTAGCAAATATTTTTGTAAGCAATT-3′	Msp I
Pro(G)1019Pro(A)	5′-CAGATCTTGAAAAGGGTTCT-3′ 5′-TCCCATGAGCTATTAGAGAAAGAATCCTTCCA-3′	Nco I
Ser(T)343Ser(C)	5′-CTTTCCACCTAAAATTCTGACAAT-3′ 5′-CATGATCACTCACAACATCATACT-3′	Mfe I

Table 2 Genotype distribution of leptin and leptin receptor genes (n = 136).

Leptin gene polymorphism locus			
(+19) A –> G	A/A	A/G	G/G
	4 (2.9%)	39 (28.7%)	93 (68.4%)
(–2548) G –> A	G/G	G/A	A/A
	7 (5.1%)	40 (29.4%)	89 (65.5%)
(–188) C –> A	C/C	C/A	A/A
	136 (100%)		
(–633) C –> T	C/C	C/T	T/T
	136 (100%)		
Leptin receptor gene polymorphism			
Lys(G)109Arg(A)	G/G	G/A	A/A
	3 (2.2%)	53 (39.0%)	80 (58.8%)
Gln(G)223Arg(A)	G/G	G/A	A/A
	4 (2.9%)	41 (30.1%)	91 (67.0%)
Pro(G)1019Pro(A)	G/G	G/A	A/A
	1 (0.7%)	40 (29.4%)	95 (69.9%)
Ser(T)343Ser(C)	T/T	T/C	C/C
	99 (72.8%)	16 (11.8%)	21 (15.4%)

Relationship between leptin/leptin receptor gene polymorphisms and serum lipid profile

Serum lipid profiles of LEPR gene polymorphism groups are shown in Table 3.The mean serum lipid levels were not statistically different among leptin/LEPR gene polymorphism groups (+19)A–>G, (–2548)G–>A, Gln223Arg, Pro1019Pro). Arg109Arg homozygotes in LEPR gene had lower TC and LDL-C levels, and the frequency of Lys109Lys homozygotes was significantly higher in the high LDL-C group ($p = 0.0060$). In addition, Ser343Ser(C/C) homozygotes in LEPR gene had lower TG levels; however, the gene polymorphism distribution was not different between hypertriglyceridaemia group and normal TG level group ($p = 0.2567$).

Interaction of leptin/leptin receptor gene polymorphisms and relative weight for serum lipids

The mean relative weights of LEPR gene polymorphism groups are shown in Table 4. No significant relationship was observed between leptin gene polymorphisms and relative weight. Among Gln223Arg and Pro1019Pro polymorphism groups in LEPR gene, no difference was demonstrated in relative weight. On the other hand, Lys109Arg and Ser343Ser polymorphisms had significant relationship with relative weight. Arg109Arg homozygotes in LEPR gene had higher relative weight, and Ser343-Ser(C/C) homozygotes in LEPR gene had lower relative weight. The gene polymorphism distribution of Lys109Arg was similar in two groups (relative weight >150 and 120–150, $p = 0.2383$). However, the frequency of Ser343-Ser(T/T) homozygotes was significantly higher in severe obesity group ($p = 0.0008$). To investigate the interaction of LEPR gene polymorphisms (Lys109Arg, Ser343Ser) and relative weight on serum lipids, multiple regression analyses were performed (Table 5). Lys109Arg polymorphism was the only significant determinant of TC and LDL-C levels. However, both relative weight and Ser343Ser polymorphism were the significant determinants of TG levels.

DISCUSSION

In mice, leptin may play a physiological role in regulating HDL-C and apolipoprotein levels (28,29). In a human twins study (30), 19A homozygotes of leptin (+19)A–>G had lower HDL-C levels. However, in this study, the significant association between leptin gene polymorphisms and serum lipids, including HDL-C levels, was not found. Therefore, our results suggested that the influence of leptin gene polymorphisms was less than other factors affecting serum lipids in obese Japanese children. In respect of LEPR gene polymorphisms, the genotype frequencies in this study were similar to the previous reports in Japanese population (15–18,24), although all our subjects were obese children. The association between LEPR

Table 4 Genotypes of leptin receptor genes and relative weight

	Relative weight (%)			p-value
Leptin receptor gene polymorphism				
Lys(G)109Arg(A)	G/G (n = 3)	G/A (n = 53)	A/A (n = 80)	0.0251
	134.4 ± 7.0	150.3 ± 2.7	160.8 ± 3.1	
Ser(T)343Ser(C)	T/T (n = 99)	T/C (n = 16)	C/C (n = 21)	0.0040
	159.8 ± 2.6	148.7 ± 4.7	144.6 ± 5.1	

Table 3 Genotypes of leptin receptor genes and serum lipid profile (Kruskal–Wallis test)

Leptin receptor gene polymorphism				
Lys(G)109Arg(A)	**G/G (n = 3)**	**G/A (n = 53)**	**A/A (n = 80)**	**p-value**
Total cholesterol (mg/dL)	186.7 ± 15.6	194.0 ± 5.7	176.2 ± 3.9	0.0196
Low density lipoprotein cholesterol (mg/dL)	121.8 ± 22.2	117.1 ± 4.6	105.1 ± 3.5	0.0402
High density lipoprotein cholesterol (mg/dL)	49.3 ± 3.4	55.2 ± 2.0	49.3 ± 1.1	0.1138
Triglyceride (mg/dL)	178.0 ± 127.0	110.6 ± 8.3	109.3 ± 6.4	0.8100
Ser(T)343Ser(C)	**T/T (n = 99)**	**T/C (n = 16)**	**C/C (n = 21)**	
Total cholesterol (mg/dL)	180.6 ± 3.7	202.3 ± 9.8	182.1 ± 8.9	0.0959
Low density lipoprotein cholesterol (mg/dL)	106.7 ± 3.0	126.1 ± 8.8	113.5 ± 8.3	0.1034
High density lipoprotein cholesterol (mg/dL)	50.8 ± 1.3	55.1 ± 3.3	52.7 ± 2.3	0.4204
Triglyceride (mg/dL)	119.0 ± 6.8	104.9 ± 15.0	79.9 ± 8.7	0.0139

Table 5 Multiple regression analyses of the relationship between indices of obesity and serum lipids

Predictor	Coefficient	SE	p-value
Total cholesterol (r = 0.255, p = 0.0115)			
Relative weight	0.231	0.132	0.0818
Lys109Arg	−17.349	6.125	0.0053
LDL-cholesterol (r = 0.222, p = 0.0358)			
Relative weight	0.158	0.112	0.1590
Lys109Arg	−13.122	5.334	0.0152
Triglyceride (r = 0.284, p = 0.0038)			
Relative weight	0.473	0.219	0.0327
Ser343Ser	−15.088	7.364	0.0425

gene polymorphisms and serum lipid profile in Japanese population has been investigated in several studies. Nishikai et al. reported that, in non-diabetic adults, HDL-C levels and apolipoprotein A-I levels were influenced by LEPR gene 3′-untranslated region polymorphism (14). Takahashi-Yasuno et al. shown that Gln223Arg polymorphism is associated with significant elevation of serum TC and LDL-C levels (24). However, in another report in Japanese adults (15), serum lipid profile did not relate with Lys109Arg or Gln223Arg polymorphisms. In addition, in Japanese children, Gln223Arg polymorphism was also reported to have no influence on serum lipids (16). In this study, we found the significant influence of Lys109Arg polymorphism on TC and LDL-C, but not on HDL-C or TG, and no effect of Gln223Arg polymorphism on each serum lipid. In the study in Thai children, Lys656Asn polymorphism of LEPR gene associated with serum lipids; high TC and LDL-C levels in Lys656Lys homozygotes (23). Thus, the locus of SNP in LEPR gene that had significant influence on serum lipids was different among the reports, probably because of the subject characteristics, such as ethnicity, sex, age and complications.

Another new finding of this study was the effect of LEPR gene polymorphisms on the degree of obesity, being observed in Lys109Arg and Ser343Ser. Several previous Japanese studies were carried out in other population including Japanese to investigate the association. However, those studies could not find the significant association of any LEPR gene polymorphism, including Lys109Arg or Ser343Ser, with obesity (15,17,18). The Gln223Arg polymorphism was investigated in Japanese children, demonstrating no association with relative weight (16). According to our results, the genotype frequencies in LEPR (Lys109Arg and Ser343Ser) of obese Japanese children were similar to the previous reports. Therefore, the influence on the degree of obesity observed in this study may depend on the interactions with other factors that deteriorate obesity. Unfortunately, we could not recruit non-obese children in this study. Therefore, case–control studies should be performed to confirm the impact of LEPR polymorphisms on relative weight and serum lipids.

In conclusion, this is the first report of the association between serum lipids and LEPR gene polymorphisms in obese Japanese children. The significant influence of Lys109Arg polymorphism in LEPR gene on both TC and LDL-C elevations was demonstrated. In addition, Lys109Arg and Ser343Ser polymorphisms were associated with the degree of obesity. Therefore, LEPR gene polymorphisms may partly contribute to the cardiovascular risks in obesity.

ACKNOWLEDGEMENTS

This study has been accomplished by the collaboration of members of The Study Group of Pediatric Obesity and Its related Metabolism. In appreciation of their efforts, listed names of the rest of members as follows: Kenji Fujieda (Asahikawa Medical College), Kohtaro Asayama (Tokyo Kasei-Gakuin University), Hiroshi Tamai (Osaka Medical College), Keiichi Hanaki (Tottori University Faculty of Medicine), Mitsuhiko Hara (Tokyo Metropolitan Hiroo Hospital), Thoru Kikuchi (Niigata University Faculty of Medicine), Junichi Kajiwara (JCR Pharmaceuticals Co., Ltd).

References

1. Kopelman PG. Obesity as a medical problem. *Nature* 2000; 404: 635–43.
2. Maes HH, Neale MC, Eaves LJ. Genetic and environmental factors in relative body weight and human adiposity. *Behav Genet* 1997; 27: 325–51.
3. Stunkard AJ, Harris JR, Pedersen NL, McClearn GE. The body-mass index of twins who have been reared apart. *N Engl J Med* 1990; 322: 1483–7.
4. Silventoinen K, Kaprio J, Lahelma E. Genetic and environmental contributions to the association between body height and educational attainment: a study of adult Finnish twins. *Behav Genet* 2000; 30: 477–85.
5. Carmichael CM, McGue M. A cross-sectional examination of height, weight, and body mass index in adult twins. *J Gerontol A Biol Sci Med Sci* 1995; 50: B237–44.
6. Swarbrick MM, Vaisse C. Emerging trends in the search for genetic variants predisposing to human obesity. *Curr Opin Clin Nutr Metab Care* 2003; 6: 369–75.
7. Farooqi IS. Monogenic human obesity. *Front Horm Res* 2008; 36: 1–11.
8. Cohen P, Friedman JM. Leptin and the control of metabolism: role for stearoyl-CoA desaturase-1 (SCD-1). *J Nutr* 2004; 134: 2455S–63S.
9. Farooqi IS, O'Rahilly S. Genetics of obesity in humans. *Endocr Rev* 2006; 27: 710–8.
10. Paracchini V, Pedotti P, Taioli E. Genetics of leptin and obesity: a HuGE review. *Am J Epidemiol* 2005; 162: 101–14.
11. van der Lende T, Te Pas MF, Veerkamp RF, Liefers SC. Leptin gene polymorphisms and their phenotypic associations. *Vitam Horm* 2005; 71: 373–404.
12. Shigemoto M, Nishi S, Ogawa Y, Isse N, Matsuoka N, Tanaka T, et al. Molecular screening of both the promoter and the protein coding regions in the human ob gene in Japanese obese subjects with non-insulin-dependent diabetes mellitus. *Eur J Endocrinol* 1997; 137: 511–3.
13. Ohshiro Y, Ueda K, Nishi M, Ishigame M, Wakasaki H, Kawashima H, et al. A polymorphic marker in the leptin gene associated with Japanese morbid obesity. *J Mol Med* 2000; 78: 516–20.

14. Nishikai K, Hirose H, Ishii T, Hayashi M, Saito I, Saruta T. Effects of leptin receptor gene 3′-untranslated region polymorphism on metabolic profiles in young Japanese men. *J Atheroscler Thromb* 2004; 11: 73–8.
15. Ogawa T, Hirose H, Yamamoto Y, Nishikai K, Miyashita K, Nakamura H, et al. Relationships between serum soluble leptin receptor level and serum leptin and adiponectin levels, insulin resistance index, lipid profile, and leptin receptor gene polymorphisms in the Japanese population. *Metabolism* 2004; 53: 879–85.
16. Endo K, Yanagi H, Hirano C, Hamaguchi H, Tsuchiya S, Tomura S. Association of Trp64Arg polymorphism of the beta3-adrenergic receptor gene and no association of Gln223Arg polymorphism of the leptin receptor gene in Japanese schoolchildren with obesity. *Int J Obes Relat Metab Disord* 2000; 24: 443–9.
17. Takahashi-Yasuno A, Masuzaki H, Miyawaki T, Matsuoka N, Ogawa Y, Hayashi T, et al. Association of Ob-R gene polymorphism and insulin resistance in Japanese men. *Metabolism* 2004; 53: 650–4.
18. Matsuoka N, Ogawa Y, Hosoda K, Matsuda J, Masuzaki H, Miyawaki T, et al. Human leptin receptor gene in obese Japanese subjects: evidence against either obesity-causing mutations or association of sequence variants with obesity. *Diabetologia* 1997; 40: 1204–10.
19. Rosmond R, Chagnon YC, Holm G, Chagnon M, Pérusse L, Lindell K, et al. Hypertension in obesity and the leptin receptor gene locus. *J Clin Endocrinol Metab* 2000; 85: 3126–31.
20. Popko K, Gorska E, Wasik M, Stoklosa A, Pywaczewski R, Winiarska M, et al. Frequency of distribution of leptin receptor gene polymorphism in obstructive sleep apnea patients. *J Physiol Pharmacol* 2007; 58(Suppl. 5): 551–61.
21. Prieur X, Tung YC, Griffin JL, Farooqi IS, O'Rahilly S, Coll AP. Leptin regulates peripheral lipid metabolism primarily through central effects on food intake. *Endocrinology* 2008; 149: 5432–9.
22. Muoio DM, Lynis Dohm G. Peripheral metabolic actions of leptin. *Best Pract Res Clin Endocrinol Metab* 2002; 16: 653–6.
23. Popruk S, Tungtrongchitr R, Petmitr S, Pongpaew P, Harnroongroj T, Pooudong S, et al. Leptin, soluble leptin receptor, lipid profiles, and LEPR gene polymorphisms in Thai children and adolescents. *Int J Vitam Nutr Res* 2008; 78: 9–15.
24. Takahashi-Yasuno A, Masuzaki H, Miyawaki T, Ogawa Y, Matsuoka N, Hayashi T, et al. Leptin receptor polymorphism is associated with serum lipid levels and impairment of cholesterol lowering effect by simvastatin in Japanese men. *Diabetes Res Clin Pract* 2003; 62: 169–75.
25. Freidewald WT, Levy RI, Fredrickson DS. Estimation of the concentration of low-density lipoprotein cholesterol in plasma, without use of the preparative ultracentrifuge. *Clin Chem* 1972; 18: 499–502.
26. Okada T, Murata M, Yamauchi K, Harada K. New criteria of normal serum lipid levels in Japanese children: the nationwide study. *Pediatr Int* 2002; 44: 596–601.
27. Asayama K, Ozeki T, Sugihara S, Ito K, Okada T, Tamai H, et al. Criteria for medical intervention in obese children: a new definition of 'obesity disease' in Japanese children. *Pediatr Int* 2003; 45: 642–6.
28. Silver DL, Wang N, Tall AR. Defective HDL particle uptake in ob/ob hepatocytes causes decreased recycling, degradation, and selective lipid uptake. *J Clin Invest* 2000; 105: 151–9.
29. Silver DL, Jiang XC, Tall AR. Increased high density lipoprotein (HDL), defective hepatic catabolism of ApoA-I and ApoA-II, and decreased ApoA-I mRNA in ob/ob mice. Possible role of leptin in stimulation of HDL turnover. *J Biol Chem* 1999; 274: 4140–6.
30. Souren NY, Paulussen AD, Steyls A, Loos RJ, Stassen AP, Gielen M, et al. Common SNPs in LEP and LEPR associated with birth weight and type 2 diabetes-related metabolic risk factors in twins. *Int J Obes (Lond)* 2008; 32: 1233–9.

Human Molecular Genetics, 2011, Vol. 20, No. 7 **1274–1284**
doi:10.1093/hmg/ddq568
Advance Access published on January 3, 2011

Wolfram syndrome 1 gene (*WFS1*) product localizes to secretory granules and determines granule acidification in pancreatic β-cells

Masayuki Hatanaka[1,2], Katsuya Tanabe[1], Akie Yanai[3], Yasuharu Ohta[1], Manabu Kondo[1], Masaru Akiyama[1], Koh Shinoda[3], Yoshitomo Oka[4] and Yukio Tanizawa[1,*]

[1]Division of Endocrinology, Metabolism, Hematological Sciences and Therapeutics, Department of Bio-Signal Analysis, [2]Department of Diabetes Research and [3]Division of Neuroanatomy, Department of Neuroscience, Yamaguchi University Graduate School of Medicine, Ube, Yamaguchi, Japan and [4]Division of Molecular Metabolism and Diabetes, Tohoku University Graduate School of Medicine, Sendai, Miyagi, Japan

Received October 15, 2010; Revised and Accepted December 29, 2010

Wolfram syndrome is an autosomal recessive disorder characterized by juvenile-onset insulin-dependent diabetes mellitus and optic atrophy. The gene responsible for the syndrome (*WFS1*) encodes an endoplasmic reticulum (ER) resident transmembrane protein. The *Wfs1*-null mouse exhibits progressive insulin deficiency causing diabetes. Previous work suggested that the function of the WFS1 protein is connected to unfolded protein response and to intracellular Ca^{2+} homeostasis. However, its precise molecular function in pancreatic β-cells remains elusive. In our present study, immunofluorescent and electron-microscopic analyses revealed that WFS1 localizes not only to ER but also to secretory granules in pancreatic β-cells. Intragranular acidification was assessed by measuring intracellular fluorescence intensity raised by the acidotrophic agent, 3-[2,4-dinitroanilino]-3′-amino-*N*-methyldipropyramine. Compared with wild-type β-cells, there was a 32% reduction in the intensity in WFS1-deficient β-cells, indicating the impairment of granular acidification. This phenotype may, at least partly, account for the evidence that *Wfs1*-null islets have impaired proinsulin processing, resulting in an increased circulating proinsulin level. Morphometric analysis using electron microscopy evidenced that the density of secretory granules attached to the plasma membrane was significantly reduced in *Wfs1*-null β-cells relative to that in wild-type β-cells. This may be relevant to the recent finding that granular acidification is required for the priming of secretory granules preceding exocytosis and may partly explain the fact that glucose-induced insulin secretion is profoundly impaired in young prediabetic *Wfs1*-null mice. These results thus provide new insights into the molecular mechanisms of β-cell dysfunction in patients with Wolfram syndrome.

INTRODUCTION

Diabetes mellitus is a heterogeneous disorder characterized by glucose intolerance that affects over 170 million people worldwide (1). The disease arises from a combination of absolute (type 1) or relative (type 2) insulin deficiency with variable peripheral insulin resistance. The failure of insulin supply is implicated to result from both impaired β-cell function and decreased β-cell mass (2–4).

Wolfram syndrome (OMIM 222300) is an autosomal recessive disorder with severe neurodegeneration. Affected individuals present with juvenile-onset insulin-dependent diabetes mellitus and optic atrophy (5). Postmortem studies of the pancreas from patients with Wolfram syndrome have revealed a selective β-cell loss (6). The gene responsible for the disorder, *WFS1*, encodes a novel transmembrane protein (7,8). The WFS1 protein, also called Wolframin, consists of 890 amino acids and is predicted to have nine membrane-spanning

*To whom correspondence should be addressed at: Division of Endocrinology, Metabolism, Hematological Sciences and Therapeutics, Yamaguchi University Graduate School of Medicine, 1-1-1 Minamikogushi, Ube, Yamaguchi 755-8505, Japan. Tel: +81 836222250; Fax: +81 836222342; Email: tanizawa@yamaguchi-u.ac.jp

domains. This protein is known to be embedded in the endoplasmic reticulum (ER) membrane (9). Mice with a disrupted *Wfs1* gene exhibit a selective β-cell loss. This phenotype has been thought to result from the activation of ER stress, impaired cell cycle progression and apoptosis (10–14). In addition, insulin secretion from the isolated islets of *Wfs1*-null mice was shown to be impaired (15). An early study has shown that WFS1 might serve directly as a divalent ion channel or, alternatively, as a regulator of existing channel activity (16). Later, it was demonstrated that WFS1 positively modulates the Ca^{2+} level in ER by increasing the rate of Ca^{2+} uptake (10). However, the lack of distinct domains in WFS1 makes it difficult to understand its precise physiological function in pancreatic β-cells.

Secretory granules are acidified through a proton gradient, established and maintained by coordinated action between H^+-pumping vacuolar-type ATPase (V-ATPase) (17) and ClC-3, a chloride ion channel (18). The low pH of late secretory granules is necessary for proinsulin processing, and in addition, for the priming of the granules preceding exocytosis (18).

In this study, WFS1 was found to localize not only in ER but also in dense-core secretory granules in pancreatic β-cells. *Wfs1*-null mice exhibited severely impaired insulin secretion in response to glucose. These observations prompted us to investigate the functional significance of the granule-resident WFS1 protein, including its role in the acidification of insulin secretory granules, as an additional physiological function of WFS1.

RESULTS

WFS1 protein localizes to insulin secretory granules

Previous studies have shown that the majority of WFS1-immunoreactive cells were insulin-producing β-cells (16,19) in pancreatic islets. However, the precise intracellular localization of WFS1 in β-cells has not been examined, whereas this protein is thought to localize predominantly in ER in WFS1-overexpressing heterologous cells (7,9,11,20). We thus attempted to detail its intracellular localization to obtain a clue to understand further physiological roles of WFS1 in pancreatic β-cells. Immunohistochemical analysis of pancreatic sections from wild-type (*Wt*) animals using anti-WFS1 antibodies and antibodies against markers for either ER or secretory granules was performed. As shown in Figure 1A–C, only a little part of the immunoreactive area for WFS1 protein (red) appeared to merge with that for Grp78, an ER marker (green). Surprisingly, there appeared to be better co-localization of WFS1 protein with chromogranin A (green), a marker of secretory granules (Fig. 1D–F). To further substantiate the localization of WFS1 protein to the secretory granule, immunoelectron microscopy using anti-WFS1 antibodies was performed. β-Cells could be distinguished from α- and δ-cells by the appearance of the secretory granules. β-Cell granules have a white halo, which is not apparent in α- and δ-granules. As described previously (19), immunoreactivity for WFS1 protein was observed in β-cells but not in α-cells (Fig. 1G). As shown in Figure 1H, there appeared to be the accumulation of immunoreactivity not only in ER but also in dense-core granules in *Wt* β-cells. High magnification more clearly showed accumulation of immunoreactivity in the periphery of electron-dense-core granules accompanied by a halo in *Wt* β-cells (Fig. 1I). Consistently, no immunoreactivity for WFS1 was observed in WFS1-deficient β-cells (Fig. 1J). These results clearly demonstrate that WFS1 localizes not only in ER but also in secretory granules in pancreatic β-cells. The intracellular distribution of WFS1 in pancreatic β-cells was assessed by immunogold electron microscopic analysis (Fig. 1K–M). We quantified the labeling by counting gold particles per β-cell area and found ~40% more immunogold particles in secretory granules relative to those in ER (Fig. 1M). No particles were found in mitochondria. From these immunohistological observations at the tissue and ultrastructural levels, we concluded that WFS1 preferentially localizes in dense-core granules in pancreatic β-cells.

WFS1 deficiency impairs intragranular acidification

Of interest to the function of WFS1, despite a lack of distinct domains in WFS1, it has nine membrane-spanning domains, enabling us to expect that this protein may function as an ion-channel regulator. We hypothesized that WFS1 in insulin granules might play a role in the regulation of acidification of insulin granules. To test this hypothesis, granular acidification was examined by incubating mechanically dispersed islet cells with the acidotrophic agent 3-[2,4-dinitroanilino]-3′-amino-*N*-methyldipropyramine (DAMP) (21,22). Insulin-producing cells were selected by co-staining for insulin. Indirect immunofluorescence intensity, raised by DAMP accumulation, in the whole cell with the exception of the nucleus was measured. The number of lysosomes in β-cells is negligible compared with insulin granules (estimated as 48 and 11 000 per β-cell, respectively) (17) and, therefore, will not significantly contribute to the fluorescent signal. Indirect immunofluorescence intensity for DAMP (green) in insulin immunoreactive cells from *Wfs1*$^{-/-}$ mice appeared to be weaker than that in insulin immunoreactive cells from *Wt* mice (Fig. 2A–I). *Wfs1*$^{-/-}$ β-cells had significantly reduced immunofluorescence intensity to an average of 68% of the average intensity of *Wt* β-cells (Fig. 2J). *Wt* β-cells incubated with bafilomycin A1, a V-ATPase inhibitor, exhibited an even larger reduction in intensity. These observations were replicated when granular acidification was assessed using LysoTracker, another acidotrophic probe (Fig. 2K). Hence, these results strongly suggest that WFS1 plays a role in maintenance of acidification in dense-core granules of pancreatic β-cells.

Islets from WFS1-deficient mice have impaired insulin processing

Processing of proinsulin into mature insulin requires cleavage by the prohormone convertase enzymes, PC1/3 and PC2 (23–25). These enzymes have an acidic optimum pH (23), and the conversion of proinsulin to insulin is strictly dependent on a low pH (24,26). We thus hypothesized that proinsulin conversion to insulin might be affected by impaired intragranular acidification in WFS1-deficient β-cells. To test this hypothesis, the amounts of insulin and proinsulin in isolated islets

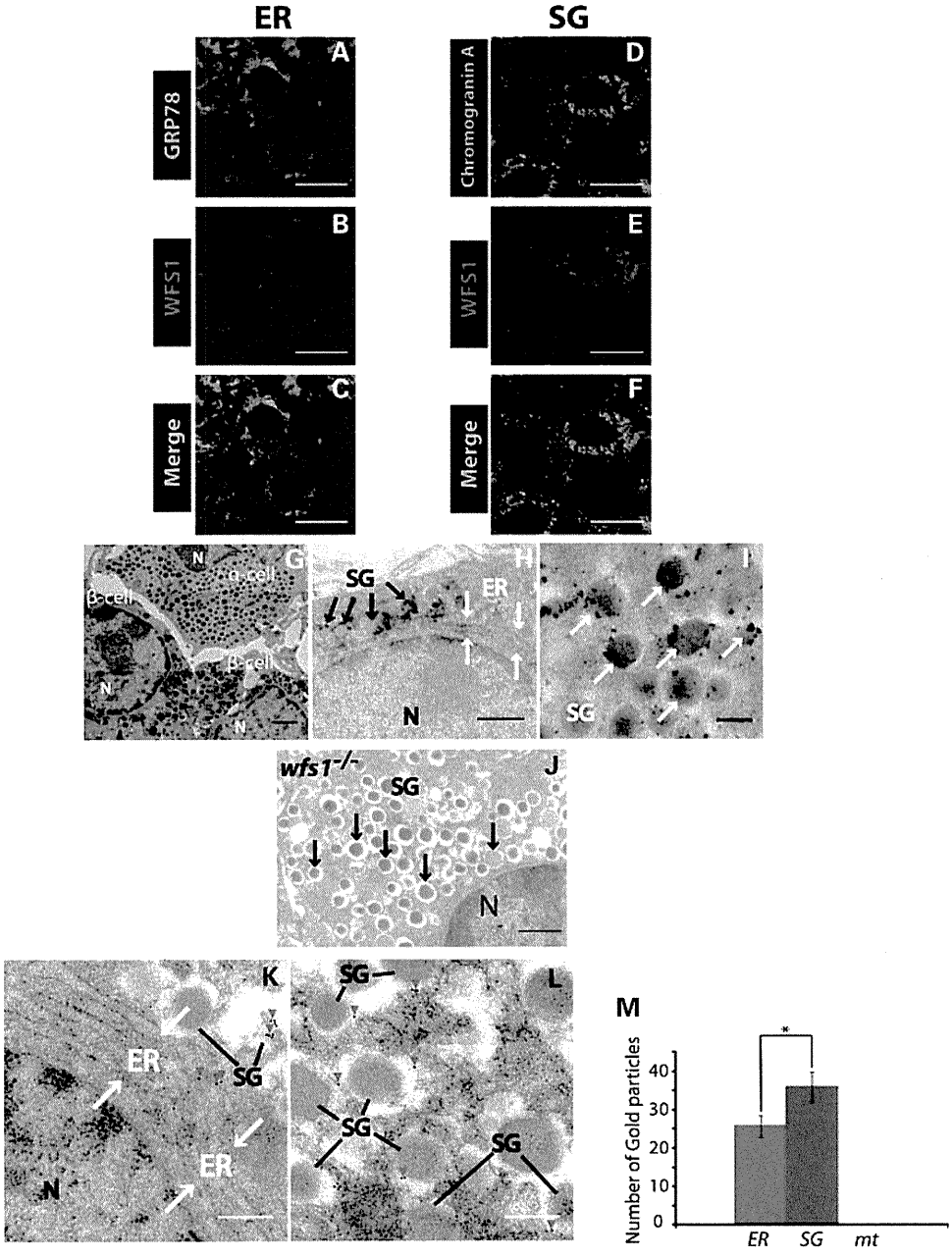

Figure 1. Localization of WFS1 to secretory granules (SG) in pancreatic β-cells. (**A**–**F**) Immunofluorescence analysis of pancreatic islets of *Wt* mice using antibodies to WFS1 (B and E, red) and antibodies to either GRP78 (A, green) or chromogranin A (D, green). Scale bars represent 10 μm. Immunoelectron microscopy of WFS1 with the DAB method, performed on pancreatic sections from *Wfs1*$^{-/-}$ and *Wt* mice (**G**–**J**). (G) Representative electron micrograph showing the localization of WFS1 in β-cells but not in α-cells. Scale bar represents 1 μm. Red arrow heads indicate WFS1 immunoreactivity. (H) Representative areas of β-cell from *Wt* mice. Scale bars represent 500 nm. (I) High magnification of representative dense-core secretory granules in β-cell from *Wt* mice. Scale bar represents 200 nm. (J) Representative area of β-cell from *Wfs1*$^{-/-}$ mice. Scale bars represent 500 nm. (**K** and **L**) Distribution of WFS1 in pancreatic β-cells. The distribution of WFS1 is shown by immunogold labeling (red arrow heads indicate examples). Bar: 200 nm. (**M**) Gold particle frequency in ER and SG per β-cell area (36 μm^2 × 24 sections). SG, secretory granule; ER, endoplasmic reticulum; mt, mitochondria.

from mice at 12 weeks of age were examined by western blot. As shown in Fig. 3A, there was a significant reduction in the abundance of mature insulin relative to GAPDH, a control for protein loading, in *Wfs1*$^{-/-}$ islets compared with that in *Wt* mice (Fig. 3B), whereas the proinsulin level was not altered (Fig. 3C). There was a consistent parallel increase in the proinsulin to insulin ratio in *Wfs1*$^{-/-}$ islets relative to that in *Wt* islets (Fig. 3D), indicating that the lack of WFS1 causes impaired insulin processing. In accordance with this observation, the plasma proinsulin level after 6 h fasting was higher in WFS1-deficient mice than in *Wt* mice (Table 1). Expression levels of prohormone convertases were further examined. As shown in Figure 3E, there was a significant reduction in the PC1/3 level in *Wfs1*$^{-/-}$ islets relative to

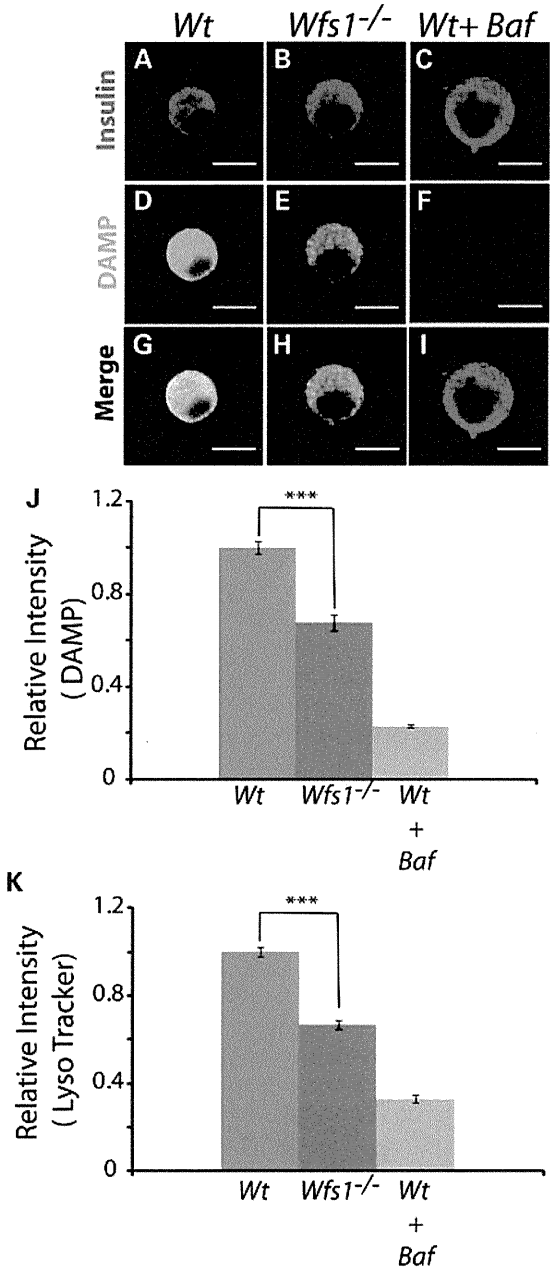

Figure 2. Disturbed intragranular acidification in WFS1-deficient β-cells. Dispersed islet cells from *Wfs1*$^{-/-}$ and *Wt* mice were incubated with either 3 μM DAMP or 25 nM LysoTracker for 1 h or 30 min, respectively, and were then fixed. (**A**–**I**) Representative photographs of DAMP-incubated islet cells stained with antibodies to DNP (green) and insulin (red). Treatment of *Wt* islet cells with bafilomycin A1 was a control of disturbed intragranular acidification. (**J**) Mean fluorescence intensity of DNP per area of each insulin-immunoreactive cell was measured. The results were obtained from 76 randomly selected *Wfs1*$^{-/-}$ β-cells and 65 *Wt* β-cells from nine different animals of each genotype. Relative intensity was expressed as the mean ± SEM. ***$P < 0.001$. (**K**) Relative mean fluorescence intensity of LysoTracker per area of each insulin-immunoreactive cell was calculated in a total of 167 *Wt* β-cells and 170 *Wfs1*$^{-/-}$ β-cells from six different animals of each genotype and graphically expressed as the mean ± SEM. ***$P < 0.001$.

that in *Wt* islets, whereas the PC2 level was not altered (Fig. 3F and G). In *Wfs1* haploinsufficiency (*Wfs1*$^{+/-}$) islets, no appreciable changes were observed in either proinsulin processing or PC1/3 expression (data not shown). To further examine the mechanism linking the lack of WFS1 to the reduced PC1/3 level, immunoprecipitation analysis using anti-WFS1 antibody was performed. However, a direct interaction of WFS1 with PC1/3 was not proved (data not shown).

WFS1 plays a role in regulation of insulin secretion *in vivo*

It has been documented that islets isolated from *Wfs1*$^{-/-}$ mice exhibited a decrease in insulin secretion in response to glucose (15). We further examined the effect of lack of WFS1 on *in vivo* insulin secretion in response to glucose at 12 weeks of age. At this age, the non-fasting blood glucose level of *Wfs1*$^{-/-}$ mice was similar to that of *Wt* mice (Fig. 4A). Glucose tolerance tests were then conducted. Blood glucose levels after overnight fasting were indistinguishable between the mutant mice and the *Wt* mice. The blood glucose level at 60 min after intraperitoneal glucose injection in WFS1-deficient mice was slightly but significantly increased relative to that in *Wt* mice (Fig. 4B). Insulin secretory response to glucose was then assessed. Whereas there was no significant change in the insulin level after overnight fasting, serum insulin levels at 2 and 15 min after glucose challenge were markedly reduced in *Wfs1*$^{-/-}$ mice compared with those in *Wt* mice. The reduced insulin levels in *Wfs1*$^{-/-}$ mice persisted until 30 min after glucose injection (Fig. 4C).

The effect of WFS1 deficiency on the β-cell mass at this age was examined. As shown in Figure 4D, insulin-positive cells still appeared to be maintained in 12-week-old WFS1-deficient mice. The insulin-immunoreactive area in WFS1-deficient mice was indistinguishable from that in *Wt* mice (Fig. 4E). Consistently, whole pancreatic insulin content was maintained in WFS1-deficient mice compared with that in *Wt* mice (Fig. 4F). These results indicate that WFS1-deficient mice have severely impaired insulin secretion in response to glucose, when abundance of β-cells is still maintained, before progressive β-cell loss becomes apparent.

WFS1 deficiency results in reduction in plasma membrane-attached secretory granules in pancreatic β-cells

To further examine the effects of WFS1 deficiency, the morphological characteristics of dense-core granules were studied by an electron microscopic analysis of pancreatic sections from randomly fed 12-week-old mice. There were no apparent differences in the appearance of electron-dense-core granules between *Wfs1*-null and *Wt* β-cells, whereas mild dilatation of ER was shown in some WFS1-deficient β-cells, as described previously (11,14) (Fig. 5A). There was no significant difference in granule size assessed by measuring granule diameter (Fig. 5B). Granule density (granule number per cytosolic area) was not affected in WFS1-deficient β-cells (Fig. 5C), either. On the other hand, the density of insulin granules docking to the plasma membrane appeared to be decreased. In fact, the number of insulin granules directly attached to the plasma membrane per cytosolic area (Fig. 5E) and per granule density (Fig. 5F) was significantly reduced in *Wfs1*$^{-/-}$ β-cells compared with that in *Wt*

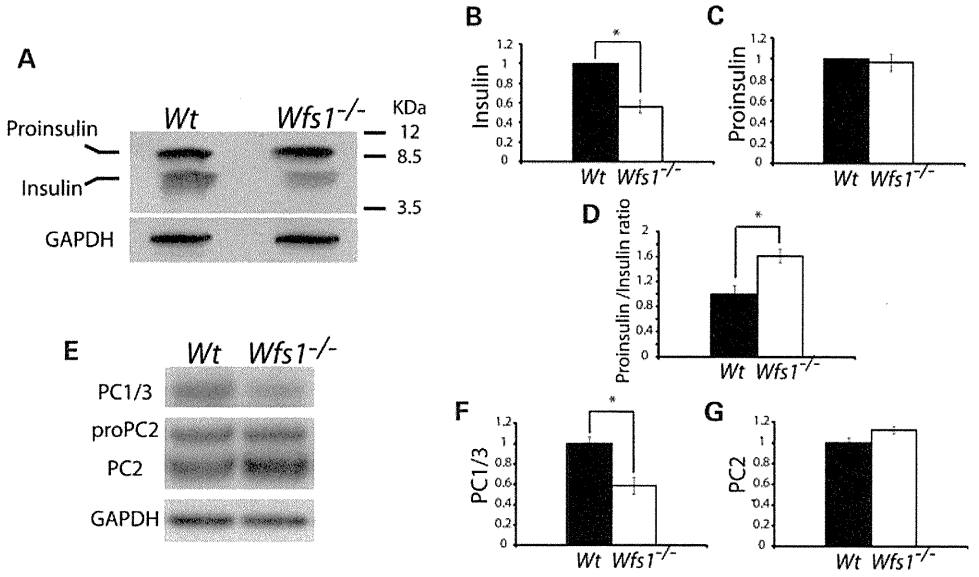

Figure 3. Impaired insulin processing in WFS1-deficient β-cells. Islets were isolated from 12-week-old *Wfs1*$^{-/-}$ and *Wt* mice. (**A**) Western blot analysis with antibodies to insulin and GAPDH. Representative results of multiple independent experiments are presented. Densities of mature insulin and proinsulin were measured and normalized to GAPDH. The results for insulin versus GAPDH (**B**), proinsulin versus GAPDH (**C**) and relative proinsulin/insulin ratio (**D**) are graphically illustrated as the mean ± SEM. $^{*}P < 0.05$. (**E**) Western blot analysis with anti-PC1, anti-PC2 and anti-GAPDH antibodies. Representative results from four independent experiments are presented. (**F** and **G**) Densities of PC1 and PC2 were measured and normalized to GAPDH. Mean protein levels ± SEM are summarized in the graph. $^{*}P < 0.05$.

β-cells. These results suggest that WFS1 function somehow determines the intracellular distribution of secretory granules, especially the docking of insulin granules to the plasma membrane. This defect may underlie, at least in part, the impairment of glucose-stimulated insulin secretion and hence may play a role in the regulation of the insulin secretory pathway.

DISCUSSION

The combination of β-cell dysfunction and β-cell loss results in progressive insulin deficiency in *Wfs1*-null mice. WFS1 has been thought to be connected with unfolded protein response and intracellular Ca^{2+} homeostasis. The present study provides additional insights into the physiological role of WFS1 in pancreatic β-cells. The following observations were documented: (i) WFS1 protein localizes in secretory granules in pancreatic β-cells; (ii) lack of WFS1 results in disturbed intragranular acidification; (iii) WFS1 deficiency causes impaired conversion of proinsulin to insulin accompanied by a decreased PC1/3 protein level; (4) WFS1-deficient β-cells have a reduced number of dense-core vesicles attached to the plasma membrane, possibly providing cellular evidence correlated with impaired insulin secretion. Taken together, these findings provide additional insights into the mechanisms of β-cell dysfunction in Wolfram syndrome.

In our present study, histological analysis at the tissue level and the ultrastructural level revealed that WFS1 was expressed not only in ER but also in dense-core granules in mouse pancreatic β-cells. In addition, immunogold particles against WFS1 were detected rather more abundantly in dense-core granules than in ER, indicating that WFS1 in dense-core granules as well as in ER could be required for sufficient β-cell function. In this regard, WFS1-deficient β-cells exhibited disturbed intragranular acidification. Because a number of membrane proteins in dense-core granules participate in important processes, such as vesicle trafficking or generation of intragranular acidification, impaired intragranular acidification is likely to result from the defect of WFS1 in dense-core granules. Intragranular acidification depends on the simultaneous operation of the V-type H^{+}-ATPase and the ClC-3 Cl^{-} channel on the insulin granule membrane (18). Although the present study did not address how WFS1 contributes to the maintenance of intragranular acidification, the function of WFS1 in insulin granules could be connected with the regulation of these channel activities.

Impaired proinsulin processing was documented in WFS1-deficient islets. Granted the impaired vesicular acidification, this is an expected and confirmatory result because acidic pH in insulin granules is required for sufficient endopeptidase activities of PC1/3 and PC2, and hence efficient proinsulin processing (23). In addition, we observed that the PC1/3 level but not the PC2 level was decreased in WFS1-deficient islets. The reduced PC1/3 level may contribute to a further reduction in endopeptidase activity of PC1/3. However, a direct link between lack of WFS1 and reduced PC1/3 level has not been proved. Exact mechanisms by which WFS1 deficiency causes reduced PC1/3 levels are unclear at this stage. Both PC1/3 and PC2 are expressed in the β-cells, whereas only PC2 is predominantly expressed in α-cells (27). If β-cells were selectively lost, decrease in PC1/3 protein would be apparent compared with PC2 in total islets. However, this is not the case because β-cell mass is not decreased at this age (Fig. 4D–F).

Secretory granules in β-cells can be divided into the readily releasable pool (RRP) and the reserve pool (28–30). The process in which granules proceed from the reserve pool

Table 1. Serum insulin and proinsulin level of 12–16-week-old mice after a 6 h fast

Genotype	Blood glucose (mg/dl)	Serum insulin (ng/ml)	Serum proinsulin (ng/ml)	Proinsulin/insulin (%)	Number
Wt	185 (±9)	0.34 (±0.03)	0.026 (±0.005)	4.6 (±0.8)	9
Wfs1$^{-/-}$	182 (±11)	0.47 (±0.05)	0.050 (±0.006)*	7.0 (±1.0)	9

*$P < 0.01$ by one-factor Student's *t*-test compared with *wt* mice.

into the RRP is referred to as mobilization and involves priming by ATP hydrolysis. A recent study demonstrated that acidification of the secretory granules is necessary for the priming of the granules preceding excytosis (18,22,31,32). We observed that the number of dense-core granules attached to the plasma membrane was reduced in β-cells of *Wfs1*-null mice, in association with impaired granular acidification. Docking and priming precede the Ca^{2+}-evoked exocytic granular fusion events, and thus this observation may explain, at least in part, the impaired glucose-stimulated insulin secretion, another pathologic feature of β-cells, in *Wfs1*-null mice.

What is the molecular function of WFS1 protein? Current information on this fundamental question is very limited. As mentioned earlier, WFS1 protein may be a channel/transporter or its functional regulator (10,16). Calcium, protons or chloride channels are candidates in ER and in the insulin secretory granules for regulation of ER calcium homeostasis or secretory granule acidification. It was also reported that WFS1 protein bound to the sodium–potassium ATPase b1 subunit (33) and calmodulin (34), although the functional significance of binding to these target molecules is unknown. Very recently, WFS1 was reported to negatively regulate activating transcription factor 6α through the ubiquitin–proteasome pathway (35). According to this finding, WFS1 may regulate target protein function, by modulating their turnover. Clearly, WFS1 can regulate multiple cellular functions and play a different role in each compartment in pancreatic β-cells.

In conclusion, previous studies have shown that WFS1 is an ER transmembrane protein that is implicated in cellular Ca^{2+} homeostasis and unfolded protein response in β-cells. Our present study has demonstrated that the WFS1 protein is also localized to the secretory granules in mouse pancreatic β-cells and suggested its functional significance. The current study provides new insights into WFS1 protein function and the pathophysiology of Wolfram syndrome.

MATERIALS AND METHODS

Animal production and metabolic phenotype analysis

Generation and genotyping of *Wfs1*$^{-/-}$ mice have been described previously (15). We maintained *Wfs1*$^{-/-}$ mice on a C57BL/6J background. For the glucose tolerance test, mice were subjected to overnight fasting followed by intraperitoneal glucose injection (2.0 g/kg). Blood glucose was measured at 0, 15, 30 and 60 min after injection using an automatic blood glucose meter, Antsense III (Horiba, Kyoto Japan). Blood samples were collected at 0, 2, 5, 15 and 30 min after injection. Insulin levels were measured by an enzyme-linked immunosorbent assay (ELISA) kit using a rat insulin standard (Morinaga, Yokohama, Japan) or the mouse insulin ELISA kit (ALPCO, Salem, NH, USA). Proinsulin was measured by the mouse proinsulin ELISA kit (ALPCO). All the experiments were carried out in male mice and were approved by the Animal Ethics Committee of Yamaguchi University School of Medicine.

Immunofluorescent staining of pancreatic islets

Pancreata were isolated from 12-week-old *Wfs1*$^{-/-}$ mice. Isolated pancreata were fixed overnight in 4% paraformaldehyde at room temperature. Tissue was then routinely processed for paraffin embedding, and 3-μm sections were cut and mounted on glass slides. The sections were immunostained with antibodies to insulin (Dako Cytomation, CA, USA), Glucagon (Santa Cruz, CA, USA), GRP78 (BD Biosciences, San Jose, CA, USA) and chromogranin A (Santa Cruz). The antibody raised against the 290 amino acid mouse WFS1-N-terminus has been described previously (9). Cy3- or fluorescein isothiocyanate-conjugated (FITC) secondary antibodies (Jackson Immunoresearch, West Grove, PA, USA) were used for fluorescence microscopy. Images were acquired on a confocal microscope (LSM 510, Carl Zeiss).

Evaluation of intragranular acidification

Islets were mechanically dissociated as previously described (15) to obtain dispersed islet cells. Cells were allowed to adhere on polylysine-coated plastic slides (Lab-Tek Chambered Coverglass, Nalge Nunc International, NY, USA) in RPMI medium, followed by 1 h pre-incubation with or without 100 nM bafilomycin A1 (Calbiochem) prior to DAMP and LysoTracker treatment. For DAMP staining, 3 μM DAMP (Invitrogen, OR, USA) was subsequently added to the medium for 1 h, and then dispersed islet cells were fixed with 4% paraformaldehyde in phosphate-buffered saline (PBS; pH 7.4). Anti-DNP-KLH secondary antibody (Molecular Probes, West Grove, PA, USA) was used for fluorescence microscopy. For LysoTracker (Molecular Probes) staining, 25 nM LysoTracker was added to the medium for 30 min. Then dispersed islet cells were fixed with 4% paraformaldehyde in PBS (pH 7.4). To recognize insulin-containing cells, after fixation, cells were stained with anti-insulin antibodies and visualized with FITC secondary antibodies. Fluorescent images were acquired with a confocal microscope, LSM 510 (Carl Zeiss). To measure fluorescence intensity derived from either DMAP or LysoTracker, a number of insulin-positive cells were randomly selected from both genotypes. The fluorescence intensity of each whole cell with the exception of the nucleus was measured and was later quantified using ImageJ 1.38× (36).

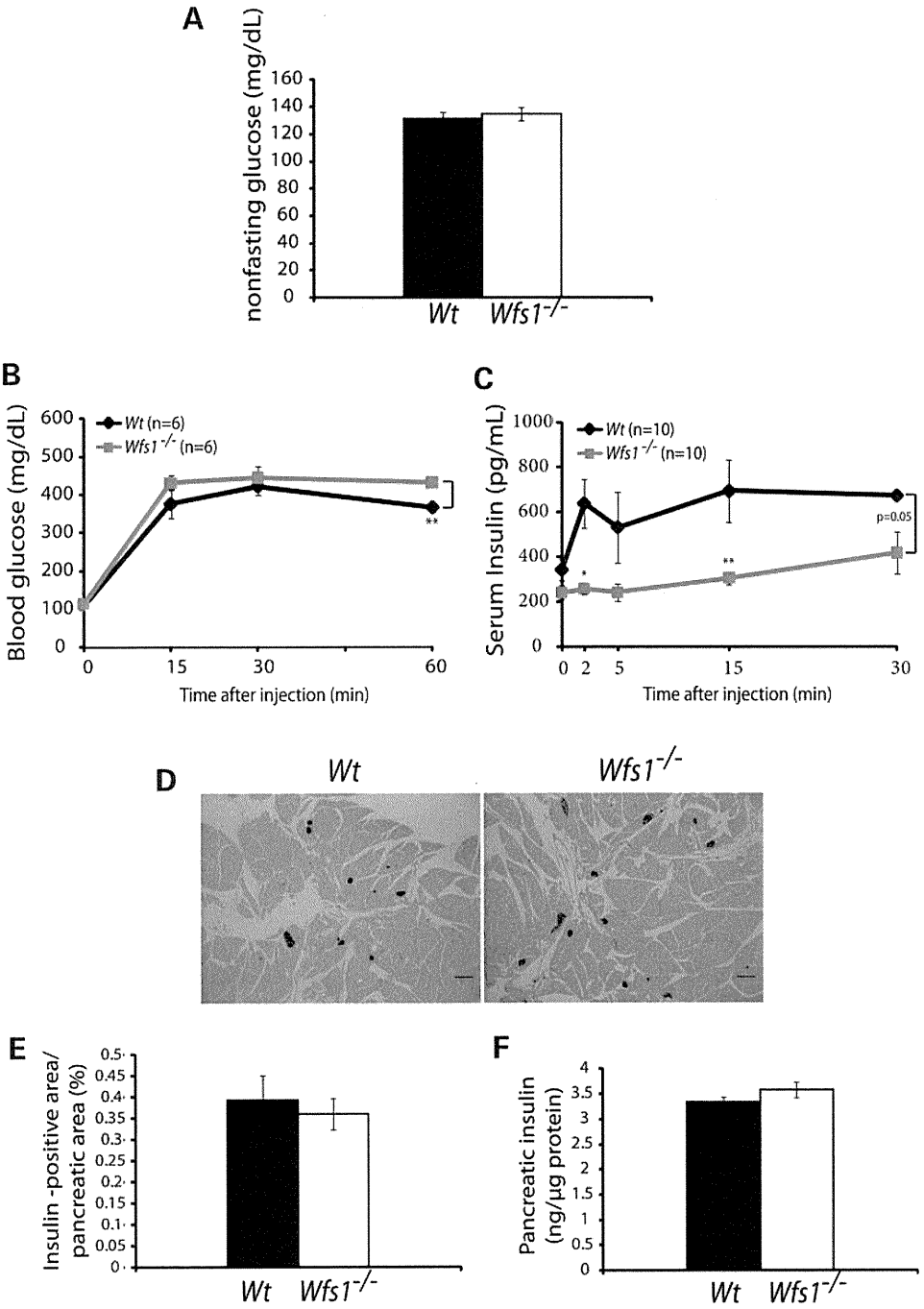

Figure 4. WFS1 deficiency results in glucose intolerance with severely impaired glucose-induced insulin release. (**A**) Non-fasting blood glucose levels in 12-week-old male mice (*Wt*, $n = 11$; *Wfs1*$^{-/-}$, $n = 11$). Intraperitoneal glucose tolerance tests were performed on overnight-fasted male *Wt* and *Wfs1*$^{-/-}$ mice at 12 weeks of age after intraperitoneal injection of D-glucose (2 g/kg) (**B** and **C**). (B) Glucose levels at the indicated time intervals. $^{*}P < 0.05$; $^{**}P < 0.01$ (*Wt*, $n = 6$; *Wfs1*$^{-/-}$, $n = 6$). (C) Plasma insulin levels at indicated time points after glucose injection (*Wt*, $n = 10$; *Wfs1*$^{-/-}$, $n = 10$). Random pancreatic sections from the entire pancreas of 12-week-old mice of the indicated genotypes were stained with antibodies to insulin and then counterstained with hematoxylin (**D** and **E**). (D) Representative photographs of indicated genotypes are shown. Scale bar represents 300 µm. (E) Insulin-immunoreactive area was measured. Results are expressed as % of total pancreatic area containing insulin-immunoreactive cells (*Wt*, $n = 3$; *Wfs1*$^{-/-}$, $n = 3$). (**F**) Insulin content extracted from whole pancreas of *Wt* and *Wfs1*$^{-/-}$ mice (*Wt*, $n = 15$; *Wfs1*$^{-/-}$, $n = 12$).

Measurement of β-cell area

All animals were anesthetized with sodium pentobarbital (65 mg/kg, intraperitoneally) and perfused intracardially with 4% paraformaldehyde. Isolated pancreatic tissues were then routinely processed for paraffin embedding, and 3 µm sections were cut and mounted on glass slides. The sections were de-paraffinized and re-hydrated, then immunostained with antibodies to insulin (Dako) bound to biotin-conjugated secondary antibodies with 3,3′-diaminobenzidine

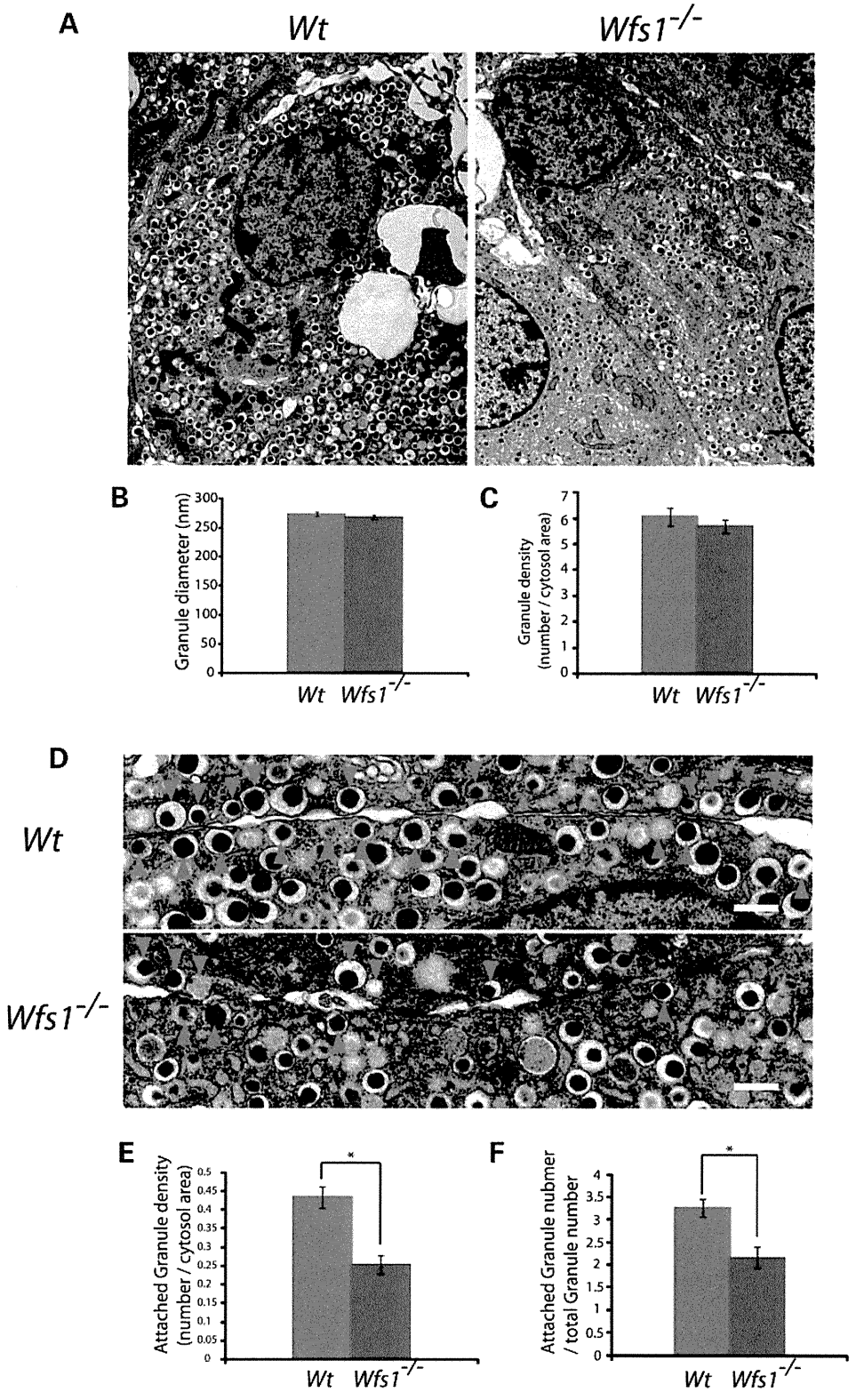

Figure 5. WFS1-deficient β-cells have reduced the number of dense-core secretory granules attached to the plasma membrane. Morphometric analyses of insulin granules in β-cells from *Wfs1*$^{-/-}$ and *Wt* mice. For each genotype, 20 randomly selected β-cells from two 12-week-old male mice were analyzed. (**A**) Electron micrographs of β-cell sections from *Wfs1*$^{-/-}$ and *Wt* mice. Scale bar represents 1 μm. (**B**) Average granule diameter and (**C**) granule number per cytosol area (μm^2). (**D**) Electron micrographs of insulin granules attached to the plasma membrane. Scale bars indicate 500 nm. (**E**) Average number of attached granules per cytosol area (μm^2) and (**F**) the attached granules to total granules ratio are summarized as the mean ± SEM in the graph. *$P < 0.05$.

tetrahydrochloride and hematoxylin. The β-cell area was determined after analysis of a number of random sections from three mice in each genotype and analyzed with ImageJ 1.38×.

Isolation of islets from mice

Islets from 12-week-old C57BL/6J male mice, *Wfs1*$^{-/-}$ and *Wfs1*$^{+/-}$/C57BL/6J background male mice were isolated by ductal collagenase digestion of the pancreas (15) followed by filtering and washing through a 70-mm Nylon cell strainer (BD Biosciences). Isolated islets were then maintained in RPMI medium containing 11 mM glucose, 10% FBS, 200 U/ml of penicillin and 200 mg/ml of streptomycin in humidified 5% CO_2 and 95% air at 37°C. All experiments on isolated islets were carried out 15 h after isolation.

Preparation of total cell extract

Isolated islets were washed twice in ice-cold PBS and lysed in ice-cold cell lysis buffer consisting of 50 mM HEPES (pH 7.5), 1% (v/v) Triton X-100, 2 mM activated sodium orthovanadate, 100 mM sodium fluoride, 10 mM sodium pyrophosphate, 4 mM EDTA, 1 mM phenylmethylsulfonyl fluoride, 1 μg/ml of leupeptin and 1 μg/ml of aprotinin, then passed through a syringe with a 21 gauge needle 10 times, and particulate material was removed by centrifugation (10 000*g* for 10 min at 4°C). The supernatant was collected. Protein concentrations were determined using the BCA protein assay (Thermo Scientific, Rockford, IL, USA).

For immunoprecipitation, mouse insulinoma MIN6 cells were cultured in 100 mm diameter culture dishes until 80% confluence and lysed in ice-cold RIPA buffer consisting of 20 mM HEPES (pH 7.2), 100 mM NaCl, 25 mM NaF, 1 mM sodium vanadate, 1 mM benzamidine, 5 μg/ml of leupeptin, 5 μg/ml of aprotinin, 1 mM phenylmethylsulfonyl fluoride, 1 mM dithiothreitol and 0.5% NP-40 in the presence of 1 mM EDTA and centrifuged for 15 min at 15 000*g*. Immunoprecipitation was performed using anti-WFS1 antibody and protein A Sepharose. After washing, immune complexes were directly eluted from the Sepharose using RIPA buffer.

Western blot analysis

Proteins were resolved on 4–20 or 15–25% gradient polyacrylamide gels (Cosmo Bio Tokyo), blotted onto a PVDF membrane (Amersham Plc, Buckinghamshire, UK) and incubated overnight at 4°C in Tris-buffered saline containing a 1:500–1000 dilution of antibodies as listed below. The membrane was then incubated at 4°C for 60 min in Tris-buffered saline with a 1:5000 dilution of anti-rabbit IgG or anti-mouse IgG horseradish peroxidase–conjugated secondary antibody (Jackson Immunoresearch). Antibodies used were anti-WFS1 (9), anti-insulin/proinsulin (Dako), anti-PC2 (Gene Tex), anti-PC1/3 (Abcam, Cambridge, UK) and anti-mGAPDH (Sigma, St Louis, MO, USA). Immune complexes were revealed using an ECL Western Blot Detection kit (Amersham Plc) and the images were acquired by exposure onto medical X-ray film (Konica Minolta). Band intensities in the blots were later quantified using ImageJ 1.38× (36), and mGAPDH bands were used to adjust for loading differences.

Electron microscopy

Conventional electron microscopy was performed as described previously (14). In brief, isolated pancreases were routinely processed. Ultrathin sections were doubly stained with uranyl acetate and lead citrate, and then observed under an electron microscope (Tecnai^{TM} G^2 Spirit, FEI Company). The diameter and the density of secretory granules were analyzed and quantified using ImageJ 1.38× (36).

Immunoelectron microscopy

All animals were anesthetized with sodium pentobarbital (65 mg/kg, intraperitoneally) and perfused intracardially with ice-cold saline, followed by 0.5% glutaraldehyde and 4% paraformaldehyde in 0.1 M phosphate buffer (PB; pH 7.4). Pancreata were removed and soaked in 0.1 M PB containing 30% sucrose until they sank, and then frozen in powdered dry ice. Pancreatic sections were cut at a thickness of 60 μm using a cryostat. The free-floating sections were pre-incubated for 2 h with 20% normal goat serum (NGS) in PBS and bleached for 1 h with 50% methanol and 1.5% hydrogen peroxide at 4°C. After washing with PBS containing 0.05% NGS and 0.3% Triton X-100, the sections were incubated with anti-WFS1 diluted 1:200 in PBS containing 1% NGS for 2 days at 20°C. Then, the sections were incubated for 2 h at 20°C with biotinylated secondary antibody (Dako Cytomation, Glostrup, Denmark; diluted 1:500) in PBS containing 1% NGS, followed by incubation with a mixture of horseradish peroxidase and rabbit anti-horseradish peroxidase antibody complexes (PAP; Dako Cytomation) and peroxidase-conjugated streptavidin (Dako Cytomation, diluted 1:500) in PBS (PAP-BAP method) for 2 h at 20°C. Subsequently, they were washed in 0.05 M Tris–HCl buffer and colored by a nickel-enhanced DAB reaction. The sections were post-fixed for 1 h with 1% OsO_4 in 0.1 M PB, block-stained for 1 h with 2% uranyl acetate in distilled water, dehydrated with a graded series of ethanol rinses, infiltrated with propylene oxide and finally embedded in epoxy resin. Ultrathin sections were collected on copper grids and observed under a Tecnai^{TM} G^2 Spirit (FEI Company) electron microscope, operated at 120 kV with 2 min of lead staining. For immune-gold-electron microscopy, the pre-embedded immunogold method was used. Cryosections (60 μm) were incubated with anti-WFS1 diluted 1:100 in PBS containing 1% NGS for 5 days at 20°C, followed by incubation with secondary antibodies conjugated with colloidal gold (10 nm diameter, BB International, diluted 1:20). Quantification of the distribution of gold particles on secretory granules and ER was performed in representative sections of a number of cells ($n = 24$).

Statistical analysis

Data were obtained from at least three independent experiments and presented as mean ± SEM. The significance of variations was analyzed by one-factor Student's *t*-test with a significance level of 0.05 (95% confidence interval).

ACKNOWLEDGEMENTS

The authors would like to thank members of the division for helpful discussion.

Conflict of Interest statement. None declared.

FUNDING

This study was supported in part by Grants-in-Aid for Scientific Research (16390096, 18390103 and 20390093 to Y.T., 22590984 to K.T., 21500326 to K.S.) from the Ministry of Education, Culture, Sports, and Science, grants (to Y.O. and Y.T.) from the Ministry of Health, Labor and Welfare of Japan, grants from the Takeda Science Foundation (to Y.T. and K.T.) and a grant from Banyu Life Science Foundation (to K.T.).

REFERENCES

1. Wild, S., Roglic, G., Green, A., Sicree, R. and King, H. (2004) Global prevalence of diabetes: estimates for the year 2000 and projections for 2030. *Diabetes Care*, **27**, 1047–1053.
2. Donath, M.Y. and Halban, P.A. (2004) Decreased beta-cell mass in diabetes: significance, mechanisms and therapeutic implications. *Diabetologia*, **47**, 581–589.
3. Rhodes, C.J. (2005) Type 2 diabetes-a matter of beta-cell life and death? *Science*, **307**, 380–384.
4. Porter, J.R. and Barrett, T.G. (2005) Monogenic syndromes of abnormal glucose homeostasis: clinical review and relevance to the understanding of the pathology of insulin resistance and beta cell failure. *J. Med. Genet.*, **42**, 893–902.
5. Barrett, T.G. and Bundey, S.E. (1997) Wolfram (DIDMOAD) syndrome. *J. Med. Genet.*, **34**, 838–841.
6. Karasik, A., O'Hara, C., Srikanta, S., Swift, M., Soeldner, J.S., Kahn, C.R. and Herskowitz, R.D. (1989) Genetically programmed selective islet beta-cell loss in diabetic subjects with Wolfram's syndrome. *Diabetes Care*, **12**, 135–138.
7. Inoue, H., Tanizawa, Y., Wasson, J., Behn, P., Kalidas, K., Bernal-Mizrachi, E., Mueckler, M., Marshall, H., Donis-Keller, H., Crock, P. *et al.* (1998) A gene encoding a transmembrane protein is mutated in patients with diabetes mellitus and optic atrophy (Wolfram syndrome). *Nat. Genet.*, **20**, 143–148.
8. Strom, T.M., Hortnagel, K., Hofmann, S., Gekeler, F., Scharfe, C., Rabl, W., Gerbitz, K.D. and Meitinger, T. (1998) Diabetes insipidus, diabetes mellitus, optic atrophy and deafness (DIDMOAD) caused by mutations in a novel gene (Wolframin) coding for a predicted transmembrane protein. *Hum. Mol. Genet.*, **7**, 2021–2028.
9. Takeda, K., Inoue, H., Tanizawa, Y., Matsuzaki, Y., Oba, J., Watanabe, Y., Shinoda, K. and Oka, Y. (2001) WFS1 (Wolfram syndrome 1) gene product: predominant subcellular localization to endoplasmic reticulum in cultured cells and neuronal expression in rat brain. *Hum. Mol. Genet.*, **10**, 477–484.
10. Takei, D., Ishihara, H., Yamaguchi, S., Yamada, T., Tamura, A., Katagiri, H., Maruyama, Y. and Oka, Y. (2006) WFS1 protein modulates the free Ca(2+) concentration in the endoplasmic reticulum. *FEBS Lett.*, **580**, 5635–5640.
11. Riggs, A.C., Bernal-Mizrachi, E., Ohsugi, M., Wasson, J., Fatrai, S., Welling, C., Murray, J., Schmidt, R.E., Herrera, P.L. and Permutt, M.A. (2005) Mice conditionally lacking the Wolfram gene in pancreatic islet beta cells exhibit diabetes as a result of enhanced endoplasmic reticulum stress and apoptosis. *Diabetologia*, **48**, 2313–2321.
12. Yamada, T., Ishihara, H., Tamura, A., Takahashi, R., Yamaguchi, S., Takei, D., Tokita, A., Satake, C., Tashiro, F., Katagiri, H. *et al.* (2006) WFS1-deficiency increases endoplasmic reticulum stress, impairs cell cycle progression and triggers the apoptotic pathway specifically in pancreatic beta-cells. *Hum. Mol. Genet.*, **15**, 1600–1609.
13. Fonseca, S.G., Fukuma, M., Lipson, K.L., Nguyen, L.X., Allen, J.R., Oka, Y. and Urano, F. (2005) WFS1 is a novel component of the unfolded protein response and maintains homeostasis of the endoplasmic reticulum in pancreatic beta-cells. *J. Biol. Chem.*, **280**, 39609–39615.
14. Akiyama, M., Hatanaka, M., Ohta, Y., Ueda, K., Yanai, A., Uehara, Y., Tanabe, K., Tsuru, M., Miyazaki, M., Saeki, S. *et al.* (2009) Increased insulin demand promotes while pioglitazone prevents pancreatic beta cell apoptosis in WFS1 knockout mice. *Diabetologia*, **52**, 653–663.
15. Ishihara, H., Takeda, S., Tamura, A., Takahashi, R., Yamaguchi, S., Takei, D., Yamada, T., Inoue, H., Soga, H., Katagiri, H. *et al.* (2004) Disruption of the WFS1 gene in mice causes progressive beta-cell loss and impaired stimulus-secretion coupling in insulin secretion. *Hum. Mol. Genet.*, **13**, 1159–1170.
16. Osman, A.A., Saito, M., Makepeace, C., Permutt, M.A., Schlesinger, P. and Mueckler, M. (2003) Wolframin expression induces novel ion channel activity in endoplasmic reticulum membranes and increases intracellular calcium. *J. Biol. Chem.*, **278**, 52755–52762.
17. Schoonderwoert, V.T. and Martens, G.J. (2001) Proton pumping in the secretory pathway. *J. Membr. Biol.*, **182**, 159–169.
18. Barg, S., Huang, P., Eliasson, L., Nelson, D.J., Obermuller, S., Rorsman, P., Thevenod, F. and Renstrom, E. (2001) Priming of insulin granules for exocytosis by granular Cl(-) uptake and acidification. *J. Cell. Sci.*, **114**, 2145–2154.
19. Ueda, K., Kawano, J., Takeda, K., Yujiri, T., Tanabe, K., Anno, T., Akiyama, M., Nozaki, J., Yoshinaga, T., Koizumi, A. *et al.* (2005) Endoplasmic reticulum stress induces WFS1 gene expression in pancreatic beta-cells via transcriptional activation. *Eur. J. Endocrinol.*, **153**, 167–176.
20. Hofmann, S., Philbrook, C., Gerbitz, K.D. and Bauer, M.F. (2003) Wolfram syndrome: structural and functional analyses of mutant and wild-type Wolframin, the WFS1 gene product. *Hum. Mol. Genet.*, **12**, 2003–2012.
21. Anderson, R.G., Falck, J.R., Goldstein, J.L. and Brown, M.S. (1984) Visualization of acidic organelles in intact cells by electron microscopy. *Proc. Natl Acad. Sci. USA*, **81**, 4838–4842.
22. Louagie, E., Taylor, N.A., Flamez, D., Roebroek, A.J., Bright, N.A., Meulemans, S., Quintens, R., Herrera, P.L., Schuit, F., Van de Ven, W.J. *et al.* (2008) Role of furin in granular acidification in the endocrine pancreas: identification of the V-ATPase subunit Ac45 as a candidate substrate. *Proc. Natl Acad. Sci. USA*, **105**, 12319–12324.
23. Davidson, H.W., Rhodes, C.J. and Hutton, J.C. (1988) Intraorganellar calcium and pH control proinsulin cleavage in the pancreatic beta cell via two distinct site-specific endopeptidases. *Nature*, **333**, 93–96.
24. Smeekens, S.P., Montag, A.G., Thomas, G., Albiges-Rizo, C., Carroll, R., Benig, M., Phillips, L.A., Martin, S., Ohagi, S., Gardner, P. *et al.* (1992) Proinsulin processing by the subtilisin-related proprotein convertases furin, PC2, and PC3. *Proc. Natl Acad. Sci. USA*, **89**, 8822–8826.
25. Zhu, X., Orci, L., Carroll, R., Norrbom, C., Ravazzola, M. and Steiner, D.F. (2002) Severe block in processing of proinsulin to insulin accompanied by elevation of des-64,65 proinsulin intermediates in islets of mice lacking prohormone convertase 1/3. *Proc. Natl Acad. Sci. USA*, **99**, 10299–10304.
26. Orci, L., Halban, P., Perrelet, A., Amherdt, M., Ravazzola, M. and Anderson, R.G. (1994) pH-independent and -dependent cleavage of proinsulin in the same secretory vesicle. *J. Cell. Biol.*, **126**, 1149–1156.
27. Guest, P.C., Abdel-Halim, S.M., Gross, D.J., Clark, A., Poitout, V., Amaria, R., Ostenson, C.G. and Hutton, J.C. (2002) Proinsulin processing in the diabetic Goto-Kakizaki rat. *J. Endocrinol.*, **175**, 637–647.
28. Renstrom, E., Eliasson, L., Bokvist, K. and Rorsman, P. (1996) Cooling inhibits exocytosis in single mouse pancreatic B-cells by suppression of granule mobilization. *J. Physiol.*, **494** (Pt 1), 41–52.
29. Renstrom, E., Eliasson, L. and Rorsman, P. (1997) Protein kinase A-dependent and -independent stimulation of exocytosis by cAMP in mouse pancreatic B-cells. *J .Physiol.*, **502** (Pt 1), 105–118.
30. Eliasson, L., Renstrom, E., Ding, W.G., Proks, P. and Rorsman, P. (1997) Rapid ATP-dependent priming of secretory granules precedes Ca(2+)-induced exocytosis in mouse pancreatic B-cells. *J. Physiol.*, **503** (Pt 2), 399–412.
31. Deriy, L.V., Gomez, E.A., Jacobson, D.A., Wang, X., Hopson, J.A., Liu, X.Y., Zhang, G., Bindokas, V.P., Philipson, L.H. and Nelson, D.J. (2009) The granular chloride channel ClC-3 is permissive for insulin secretion. *Cell Metab.*, **10**, 316–323.
32. Li, D.Q., Jing, X., Salehi, A., Collins, S.C., Hoppa, M.B., Rosengren, A.H., Zhang, E., Lundquist, I., Olofsson, C.S., Morgelin, M. *et al.* (2009) Suppression of sulfonylurea- and glucose-induced insulin secretion in

vitro and in vivo in mice lacking the chloride transport protein ClC-3. *Cell Metab.*, **10**, 309–315.
33. Zatyka, M., Ricketts, C., da Silva Xavier, G., Minton, J., Fenton, S., Hofmann-Thiel, S., Rutter, G.A. and Barrett, T.G. (2008) Sodium-potassium ATPase 1 subunit is a molecular partner of Wolframin, an endoplasmic reticulum protein involved in ER stress. *Hum. Mol. Genet.*, **17**, 190–200.
34. Yurimoto, S., Hatano, N., Tsuchiya, M., Kato, K., Fujimoto, T., Masaki, T., Kobayashi, R. and Tokumitsu, H. (2009) Identification and characterization of Wolframin, the product of the wolfram syndrome gene (WFS1), as a novel calmodulin-binding protein. *Biochemistry*, **48**, 3946–3955.
35. Fonseca, S.G., Ishigaki, S., Oslowski, C.M., Lu, S., Lipson, K.L., Ghosh, R., Hayashi, E., Ishihara, H., Oka, Y., Permutt, M.A. *et al.* (2000) Wolfram syndrome 1 gene negatively regulates ER stress signaling in rodent and human cells. *J. Clin. Invest.*, **120**, 744–755.
36. Girish, V. and Vijayalakshmi, A. (2004) Affordable image analysis using NIH Image/ImageJ. *Indian J. Cancer*, **41**, 47.

Glucose and Fatty Acids Synergize to Promote B-Cell Apoptosis through Activation of Glycogen Synthase Kinase 3β Independent of JNK Activation

Katsuya Tanabe[1], Yang Liu[1], Syed D. Hasan[1], Sara C. Martinez[1], Corentin Cras-Méneur[1], Cris M. Welling[1], Ernesto Bernal-Mizrachi[1], Yukio Tanizawa[3], Christopher J. Rhodes[4], Erik Zmuda[5], Tsonwin Hai[5], Nada A. Abumrad[2], M. Alan Permutt[1]*

1 Division of Endocrinology, Metabolism, and Lipid Research, Washington University School of Medicine, St. Louis, Missouri, United States of America, **2** Division of Nutritional Science, Department of Medicine, Washington University School of Medicine, St. Louis, Missouri, United States of America, **3** Division of Endocrinology, Metabolism, Hematological Sciences and Therapeutics Department of Bio-Signal Analysis, Yamaguchi University Graduate School of Medicine, Ube, Yamaguchi, Japan, **4** Department of Medicine, Kovler Diabetes Center, University of Chicago, Chicago, Illinois, United States of America, **5** Department of Molecular and Cellular Biochemistry, Center for Molecular Neurobiology, Ohio State University, Columbus, Ohio, United States of America

Abstract

Background: The combination of elevated glucose and free-fatty acids (FFA), prevalent in diabetes, has been suggested to be a major contributor to pancreatic β-cell death. This study examines the synergistic effects of glucose and FFA on β-cell apoptosis and the molecular mechanisms involved. Mouse insulinoma cells and primary islets were treated with palmitate at increasing glucose and effects on apoptosis, endoplasmic reticulum (ER) stress and insulin receptor substrate (IRS) signaling were examined.

Principal Findings: Increasing glucose (5–25 mM) with palmitate (400 μM) had synergistic effects on apoptosis. Jun NH2-terminal kinase (JNK) activation peaked at the lowest glucose concentration, in contrast to a progressive reduction in IRS2 protein and impairment of insulin receptor substrate signaling. A synergistic effect was observed on activation of ER stress markers, along with recruitment of SREBP1 to the nucleus. These findings were confirmed in primary islets. The above effects associated with an increase in glycogen synthase kinase 3β (Gsk3β) activity and were reversed along with apoptosis by an adenovirus expressing a kinase dead Gsk3β.

Conclusions/Significance: Glucose in the presence of FFA results in synergistic effects on ER stress, impaired insulin receptor substrate signaling and Gsk3β activation. The data support the importance of controlling both hyperglycemia and hyperlipidemia in the management of Type 2 diabetes, and identify pancreatic islet β-cell Gsk3β as a potential therapeutic target.

Citation: Tanabe K, Liu Y, Hasan SD, Martinez SC, Cras-Méneur C, et al. (2011) Glucose and Fatty Acids Synergize to Promote B-Cell Apoptosis through Activation of Glycogen Synthase Kinase 3β Independent of JNK Activation. PLoS ONE 6(4): e18146. doi:10.1371/journal.pone.0018146

Editor: Kathrin Maedler, University of Bremen, Germany

Received July 6, 2010; **Accepted** February 27, 2011; **Published** April 26, 2011

Funding: This work was supported by National Institutes of Health (NIH) grants R37 DK16746 to M.A. Permutt, R01 DK33301 to N.A. Abumrad, RO1 DK64938 to T. Hai, NIH P60 DK20579 to the Washington University DRTC, and NIH P30DK056341 to the Adipocyte Biology and Molecular Nutrition Core of the Nutrition Obesity Research Center. Katsuya Tanabe was granted from Grants-in-Aid for Scientific Research (22590984) from Ministry of Education, Culture, Sports and Science, a grant from Takeda Science Foundation and a grant from Banyu Life Science Foundation Japan. The funders had no role in study design, data collection and analysis, decision to publish, or preparation of the manuscript.

Competing Interests: The authors have declared that no competing interests exist.

* E-mail: apermutt@dom.wustl.edu

Introduction

The natural history of Type 2 diabetes mellitus (T2D) includes a progressive decline in β-cell function associated with peripheral insulin resistance. The β-cell dysfunction has been attributed in part to loss of β-cell mass via apoptosis [1] with inadequate insulin secretion leading to hyperglycemia and other diabetes symptoms [2]. Insulin resistance is at the core of obesity associated diabetes and is thought to reflect impaired insulin signaling due to chronically increased levels of free fatty acids (FFA). High FFA are also implicated in the reduction in β-cell mass that has been referred to as lipotoxicity. The combination of elevated glucose and FFA, or "glucolipotoxicity" that is prevalent in T2D has been suggested to be a major contributor to β-cell death [3,4,5,6].

The search for molecular mechanisms for glucose potentiation of FFA- induced β-cell dysfunction has been the subject of several recent studies (see [7] for review). One area of investigation has focused on the insulin receptor substrate-PI3K-Akt signaling pathway. The first study showing that the FFA oleate impaired insulin signaling in insulinoma cells demonstrated that the cells were protected from FFA-induced apoptosis by expressing a constitutively active Akt [8]. Several biochemical and genetic studies subsequently showed that saturated FFA could promote ER stress in insulinoma cells and in primary rodent and human islets [9,10,11,12]. More recently, it was shown that high glucose

potentiated FFA induced apoptosis by enhancing ER stress [13]. ER stress in insulinoma cells was shown to impair insulin signaling through activation of ATF3, an ER stress response protein that was implicated in suppression of IRS2 expression [14]. ATF3 is another stress inducible gene that is activated in different tissues by a variety of stresses [15].

How glucose potentiates FFA induced ER stress, reduced insulin receptor substrate signaling, and apoptosis is incompletely understood. Our recent study showed that there was a dose-dependent effect of FFA in the presence of high glucose on apoptosis in insulinoma cells and primary islets [16] that was associated with JNK activation, ER stress, and reduced insulin signaling. In the current study, we found a dose-dependent effect of glucose in the presence of palmitate on cell death that appeared to be over and above JNK activation. We observed glucose dose-dependent synergistic effects on palmitate inhibition of receptor substrate signaling and activation of Gsk3β. Co-treatment with an adenovirus expressing a kinase dead Gsk3β significantly protected β-cells from cell death. Our data support importance of Gsk3β in the synergistic effects of glucose and FFA.

Materials and Methods

Cell Culture

Mouse insulinoma cell line MIN6 (passage 24–32) were grown in monolayer cultures as described previously [17] in Dulbecco's modified Eagle's medium (Sigma Aldrich) supplemented with 15% fetal bovine serum, 50 mmol/L β-mercaptoethanol at 37°C in a humidified (5% CO_2, 95% air) atmosphere. Rat insulinoma INS-r3 cells were grown as previously described [18]. The palmitic acid (palmitate), formalin, propidium iodide, IL-1b, tunicamycin and TNFα were purchased from Sigma (Saint Louis, MO). Tauroursodeoxycholic Acid Sodium Salt (TUDCA) was purchased from CALBIOCEM (Darmstadt, Germany).

Fatty acids (FFA) Treatment of MIN6 Cells and Islets

The complete protocol was previously described [16]. Briefly a 20 mM solution of the FFA in 0.01 M NaOH was incubated at 70°C for 30 minutes. Then, 330 µL of 30% BSA and 400 µL of the free FFA/NaOH mixture was mixed together and filter sterilized with 20 mL of either the DMEM or RPMI media. The approximate molar ratio of FFA:BSA is 6:1 with 400 µM palmitate. The addition of BSA or a FFA:BSA mixture has not been shown to affect the pH of the media.

Propidium iodide/Cell Death Assay

MIN6 cells were grown on glass cover slips within the wells of a 6-well plate and incubated with either BSA alone or 400 µM both FFAs complexed with BSA for 24 hours as previously described [16]. After treating cells for 24 hours with various treatments, the cells were incubated with 10 µg/ml (1 to 1000 dilution) Propidium Iodide (PI) and 20 ug DAPI added directly to the media at 37°C, 5% CO2 for 1 hour. The medium was then removed by aspiration, and the cells were washed once with PBS and then fixed by incubation with 3.7% formaldehyde for 15 min at room temperature. After fixation, the MIN6 cells were mounted with anti-fading gel solution including DAPI (Biomeda Corporation, Foster City, CA) on to glass slides. Each condition reported represents over 3000 cells counted by randomized field selection. The percentage of cell-death is reported as the number of PI stained nuclei over the total number of nuclei stained by DAPI as quantitated by Image J software 1.37 [19].

Western blot analysis

MIN6 were washed twice in ice-cold phosphate-buffered saline and were lysed in ice-cold cell lysis buffer consisting of 50 mM HEPES (pH 7.5), 1% (v/v) Nonidet P-40, 2 mM activated sodium orthovanadate, 100 mM sodium fluoride, 10 mM sodium pyrophosphate, 4 mM EDTA, 1 mM phenylmethylsulfonyl fluoride, 1 µg/mL leupeptin, and 1 µg/mL aprotinin, then passed through syringe with a 21 gauge needle 10 times while INS-r3 cells were sonicated (Misonix, Farmingdale, NY) and particulate material from both cell lines were removed by centrifugation (10,000× g; 10 min; 4°C). The supernatants were collected. Protein concentrations were determined using the Bio-Rad protein assay (Bio-Rad, Hercules, CA).

The extracts (20 µg of total protein) were resolved on 7.5% or 4–15% gradient polyacrylamide gels and were blotted onto a nitrocellulose membrane (Bio-Rad, CA), and incubated overnight at 4°C in Tris-buffered saline containing a 1:1000–5000 dilution of antibody as listed below. The membrane was then incubated at 4°C for 60 min in Tris-buffered saline with a 1:2000 dilution of anti-rabbit IgG or anti-mouse IgG horseradish peroxidase-conjugated secondary antibody (Cell Signaling Technology). Antibodies used were anti-total Akt, anti-phospho-Akt (S473), anti-cleaved Caspase3, anti-phospho-PERK (980Thr), anti-phospho-eIF2α(51Ser), anti-total JNK1/2, anti-phospho-JNK, anti-phospho-AMPK, total AMPK, anti-phospho-ACC, anti-total ACC from Cell Signaling Technology (Beverley, MA), anti-SREBP1 from Neo Markers (Fremont, CA), anti-IRS1, anti-IRS2 from Upstate (Billerica, MA), anti-ATF3, anti-Insig1, anti-Lamin from Santa Cruz (Santa Cruz, CA) and anti-α-Tubulin and from Sigma (Saint Louis, MO).

Immune complexes were revealed using ECL Advance Western Blot Detection kit (Amersham Plc, Buckinghamshire UK) and the images were acquired using a FluoroChem 8800 digital camera acquisition system (Alpha Innotech, San Leandro, CA, USA). Band intensities in the blots were later quantified using ImageJ 1.38× [19] and α-Tubulin or β-Actin bands were used to adjust for loading differences.

Nuclear and cytoplasmic fractions from MIN6

MIN6 cells were cultured in 60-mm diameter culture dishes until 80% confluency. For isolation of nuclear extracts, the cells were then collected into microtubes, centrifuged for 20 s in a microcentrifuge, and resuspended in 200 µl of 10.0 mM Hepes, pH 7.9, containing 10.0 mM KCl, 1.5 mM $MgCl_2$, and 0.5 mM dithiothreitol. After incubation at 4°C for 15 min, the cells were lysed by passing 10 times through a 21-gauge needle. Next, the cells were centrifuged for 20s in a microcentrifuge, and the supernatant (cytoplasmic fraction) was removed and frozen in small aliquots. The pellet, which contained the nuclei, was resuspended in 150 µl of 20 mM Hepes, pH 7.9, containing 20% v/v glycerol, 0.1 M KCl, 0.2 mM EDTA, 0.5 mM dithiothreitol, and 0.5 mM phenylmethanesulfonyl fluoride and then stirred at 4°C for 30 min. The nuclear extracts were then centrifuged for 20 min at 4°C in a microcentrifuge. The supernatant was collected, aliquoted into small volumes, and stored at −80°C.

Islet isolation and culture

Islets from 12 weeks of age C57BL/6 male mice were isolated by ductal collagenase distension/digestion of the pancreas [20] followed by filtering and washing through a 70 mm Nylon cell strainer (BD Biosciences, San Jose, CA). Isolated islets were then maintained in RPMI medium containing 11 mM glucose, 10% FBS, 200 units/ml penicillin, and 200/ml streptomycin in humidified 5% CO2, 95% air at 37C. The palmitate treatments were carried out 15 hours after isolation. Adenovirus infections

A.

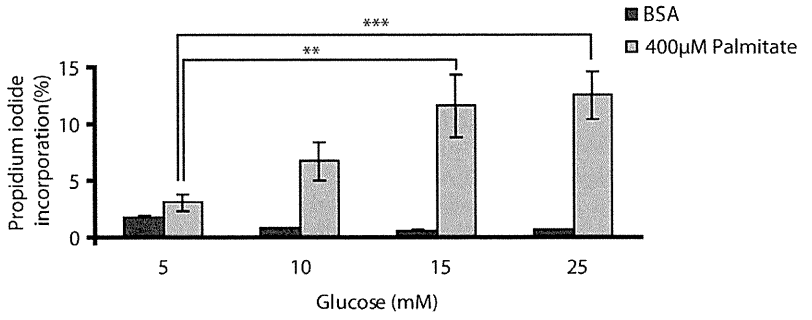
BSA
400μM Palmitate
***
**
Propidium iodide incorporation(%)
15
10
5
0
5
10
15
25
Glucose (mM)

B.

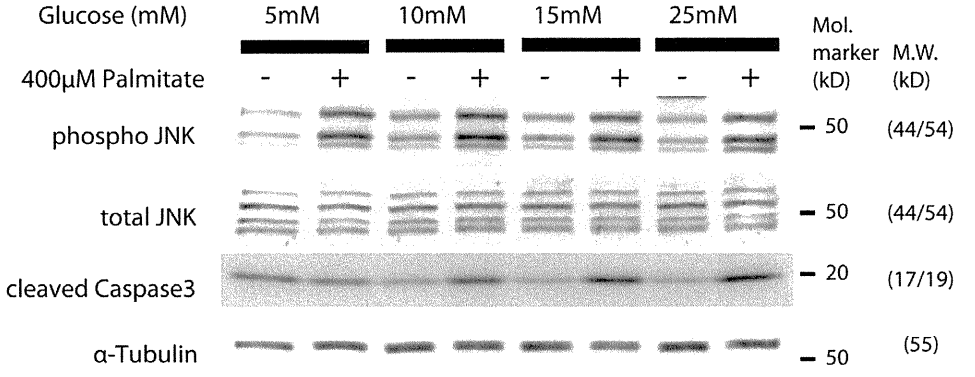
Glucose (mM)
5mM
10mM
15mM
25mM
400μM Palmitate
- + - + - + - +
Mol. marker (kD)
M.W. (kD)
phospho JNK
50
(44/54)
total JNK
50
(44/54)
cleaved Caspase3
20
(17/19)
α-Tubulin
50
(55)

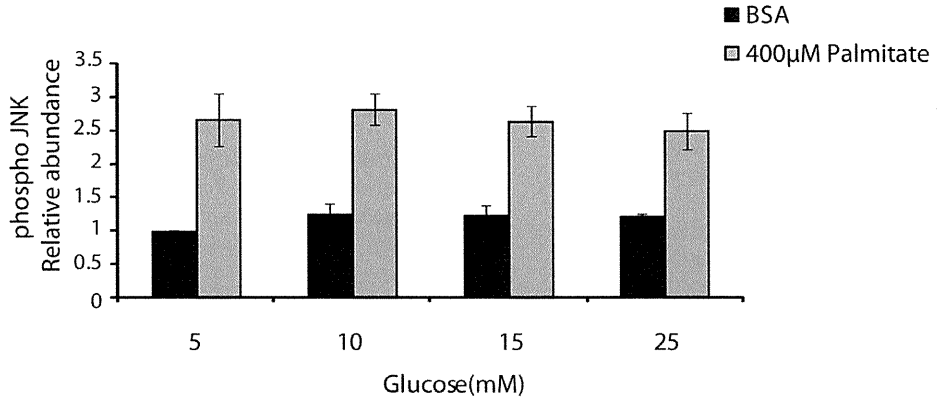
BSA
400μM Palmitate
phospho JNK Relative abundance
3.5
3
2.5
2
1.5
1
0.5
0
5
10
15
25
Glucose(mM)

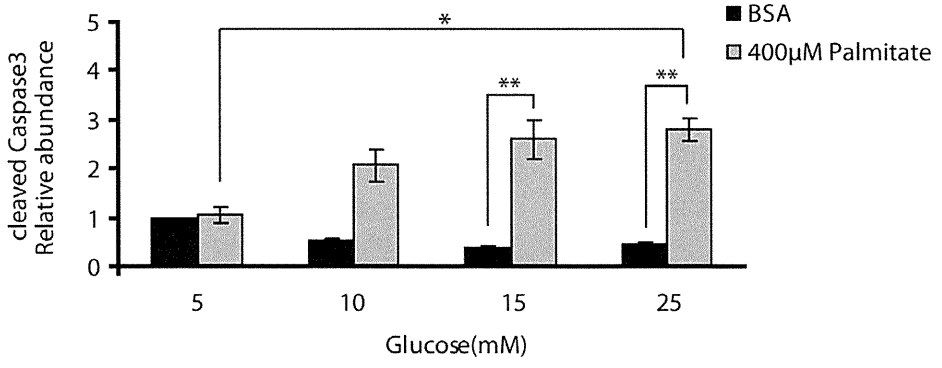
BSA
400μM Palmitate
*
**
**
cleaved Caspase3 Relative abundance
5
4
3
2
1
0
5
10
15
25
Glucose(mM)